

# **WASTE HEAT RECOVERY IN DATA CENTERS: EJECTOR HEAT PUMP ANALYSIS**

A Thesis  
Presented to  
The Academic Faculty  
By

Thomas David Harman V

In Partial Fulfillment  
of the Requirements for the Degree  
Master of Science in the  
School of Mechanical Engineering  
Georgia Institute of Technology

December 2008

# **WASTE HEAT RECOVERY IN DATA CENTERS: EJECTOR HEAT PUMP ANALYSIS**

Approved by:

**Dr. Yogendra Joshi, Advisor**  
School of Mechanical Engineering  
Georgia Institute of Technology

**Dr. S. Mostafa Ghiaasiaan**  
School of Mechanical Engineering  
Georgia Institute of Technology

**Dr. Sheldon Jeter**  
School of Mechanical Engineering  
Georgia Institute of Technology

Date Approved: October 3, 2008

## ACKNOWLEDGEMENTS

I would like to thank my advisor Dr. Yogendra Joshi for all of his assistance along the way. His guidance, patience and flexibility made it possible to accomplish all the work in this thesis. I would also like to thank my committee members Dr. Mostafa Ghiaasiaan and Dr. Sheldon Jeter for their flexibility and support.

This project could not have been completed without the support of my sponsor, Eaton Corporation. I would especially like to thank Roger Briggs, Ian Wallace and Mark Juds for their knowledge and guidance in a new an emerging area. Their long distance support and patience made this project possible.

Lastly, I would like to thank the support staff and students in the Microelectronics Thermal Laboratory. They provided insightful guidance and support when I was stumped or in need of direction. I would especially like to thank two students, Ankit Somani and Shawn Shields for assisting me in the data center activities and providing critiques and encouragement when necessary.

# TABLE OF CONTENTS

<b>WASTE HEAT RECOVERY IN DATA CENTERS: EJECTOR HEAT PUMP ANALYSIS</b>	<b>i</b>
<b>WASTE HEAT RECOVERY IN DATA CENTERS: EJECTOR HEAT PUMP ANALYSIS</b>	<b>ii</b>
<b>ACKNOWLEDGEMENTS</b>	<b>iii</b>
<b>LIST OF TABLES</b>	<b>v</b>
<b>LIST OF FIGURES</b>	<b>vi</b>
<b>LIST OF SYMBOLS</b>	<b>viii</b>
<b>LIST OF ABBREVIATIONS</b>	<b>x</b>
<b>SUMMARY</b>	<b>xi</b>
<b>1. INTRODUCTION</b>	<b>1</b>
1.1 DEVELOPING A MORE EFFICIENT DATA CENTER	1
1.2 BACKGROUND STUDY	2
1.2.1 Waste Heat Recovery Comparisons	3
1.2.2 Rack Level Cooling Technologies	11
1.3 Device Selection	13
<b>2. EJECTOR HEAT PUMP METHODS</b>	<b>14</b>
2.1 PUMP AND BOILER MODEL	15
2.2 EJECTOR MODEL	16
2.3 EJECTOR AREA AND SIZE CONSIDERATIONS	22
2.4 EVAPORATOR, CONDENSER AND THROTTLE MODELS	26
2.5 PERFORMANCE METRICS	27
2.6 EJECTOR MODEL VALIDATION	28
2.7 WORKING FLUID OPTIONS	32
2.8 WORKING FLUID SELECTION PROCESS	37
2.8.1 COP Comparisons	39
<b>3. RESULTS AND DISCUSSION</b>	<b>43</b>
3.1 BASELINE CONDITIONS	43
3.2 GEOMETRIC RELATIONSHIPS	44
3.3 COEFFICIENT OF PERFORMANCE RELATIONSHIPS	48
3.4 ECONOMIC ANALYSIS	53
3.4.1 1 MW Data Center Size Considerations	53
3.4.2 Size and Cost of Ejector Model Components	54
3.4.3 Comparison with a traditional vapor-compression system	60
<b>4. CONCLUSIONS</b>	<b>63</b>
4.1 DESIGN RECOMMENDATIONS	63
4.2 MODEL LIMITATIONS	64
4.3 MODEL IMPROVEMENTS AND FUTURE RECOMMENDATIONS	65
4.4 EJECTOR HEAT PUMP CONCLUSIONS	65
<b>INDIVIDUAL CONTRIBUTIONS</b>	<b>67</b>
<b>REFERENCES</b>	<b>69</b>

## LIST OF TABLES

TABLE 1. STATE-OF-THE-ART COMPARISONS FOR RACK LEVEL COOLING.	12
TABLE 2. VAPOR EJECTOR PROCESSES BY STATE.	22
TABLE 3. INITIAL CONDITIONS FOR R11 MODEL VALIDATION WITH THE HSU STUDY	30
TABLE 4. R11 MODEL COMPARISONS	31
TABLE 5. DETAILED COMPARISON DATA FOR EACH STATE OF THE EJECTOR HEAT PUMP CYCLE.	32
TABLE 6. FLUID SCORING MATRIX	41
TABLE 7. BASELINE OPERATING CONDITIONS FOR THE EJECTOR HEAT PUMP SYSTEM.	43
TABLE 8. SPECIFIED EJECTOR GEOMETRY BASED ON THE IDEAL, INITIAL CONDITIONS PRESENTED IN $\text{cm}^2$	44
TABLE 9. EJECTOR GEOMETRY FOR FIXED GENERATOR TEMPERATURES, PRESENTED IN $\text{cm}^2$	47
TABLE 10. MAXIMUM COP FOR GIVEN GENERATOR TEMPERATURES	52
TABLE 11. 1 MW DATA CENTER BASELINE VARIABLES FOR EACH SERVER RACK.	54
TABLE 12. FLOW RATE PER RACK FOR A HIGH DENSITY 1 MW DATA CENTER.	54
TABLE 13. BASELINE COST AND EFFECTIVENESS DATA FOR HEAT EXCHANGER ANALYSIS.	56
TABLE 14. NTU AND UA RANGE FOR HEAT EXCHANGER SIZING.	57
TABLE 15. TOTAL EJECTOR HEAT PUMP SYSTEM COST BREAKDOWN.	60
TABLE 16. CAPITAL COST COMPARISON FOR EJECTOR HEAT PUMP AND VAPOR-COMPRESSION REFRIGERATION.	60
TABLE 17. EJECTOR AND VAPOR COMPRESSION SYSTEM COST COMPARISONS	61

# LIST OF FIGURES

FIGURE 1. ABSORPTION CHILLER SCHEMATIC ILLUSTRATING THE ABSORBER CHAMBER [10]	7
FIGURE 2. ADSORPTION REFRIGERATION SYSTEM WITH TWO BED RECOVERY [10].	9
FIGURE 3. SCHEMATIC ILLUSTRATING THE THERMOMAGNETIC GENERATOR.	10
FIGURE 4. EJECTOR HEAT PUMP SCHEMATIC [HSU]	14
FIGURE 6. EJECTOR SCHEMATIC WITH STATE LOCATIONS IDENTIFIED.	16
FIGURE 7. MOLLIER DIAGRAM RELATING ALL THE PROCESSES OCCURRING IN A VAPOR EJECTOR	21
FIGURE 8. DEFINITIONS OF GEOMETRIC AREAS.	23
FIGURE 9. EJECTOR MODEL VERIFICATION, EACH POINT REPRESENTS THE STATE AS DESCRIBED IN TABLE 3.	28
FIGURE 10. ENTRAINMENT VALIDATION COMPARING THE MODEL DATA WITH THE PUBLISHED DATA.	29
FIGURE 11. R11 COMPARISON RESULTS	31
FIGURE 12. T-S DIAGRAM FOR AMMONIA, HIGHLIGHTING THE SIMILAR TRENDS AND STATE LOCATIONS TO R11	34
FIGURE 13. T-S DIAGRAM FOR R134A, HIGHLIGHTING THE SIMILAR TRENDS AND STATE LOCATIONS TO R11	35
FIGURE 14. T-S DIAGRAM FOR FC72, HIGHLIGHTING THE SIMILAR TRENDS AND STATE LOCATIONS TO R11	36
FIGURE 15. CHANGE IN EJECTOR DIAMETER OVER GIVEN TEMPERATURE RANGE	38
FIGURE 16. CHANGE IN COP OVER GIVEN TEMPERATURE RANGE	39
FIGURE 17. DEVIATION BETWEEN IDEAL AND FIXED GEOMETRY FOR $A_D$	45

FIGURE 18. ALLOWABLE GENERATOR TEMPERATURE RANGE BEFORE FREEZING OF THE EVAPORATOR WILL OCCUR.	47
FIGURE 19. DEVIATION FROM IDEAL COP AS THE GENERATOR TEMPERATURE IS REDUCED.	48
FIGURE 20. MAXIMUM ENTRAINMENT RATIO FOR A GIVEN GENERATOR TEMPERATURE.	50
FIGURE 21. MAXIMUM ATTAINABLE COP GIVEN A RISE IN $T_C$	52

## LIST OF SYMBOLS

$\Delta T$	temperature difference
$\varepsilon$	effectiveness
$\eta$	efficiency
$k$	specific heat ratio
$\lambda$	thermal conductivity
$\rho$	density
$\sigma$	electrical conductivity
$\tau$	stream temperature ratio: secondary/motive
$v$	specific volume
$A$	area
$C$	heat capacity rate
$c$	speed of sound
$c_p$	specific heat
$D$	diameter
$h$	enthalpy per unit mass
$M$	Mach number
$\dot{m}$	mass flow rate
$P$	pressure
$Q$	heat transfer
$\bar{R}$	universal gas constant
$S$	Seebeck Coefficient
$s$	entropy per unit mass
$T$	temperature
$U$	overall heat coefficient

V	velocity
W	work
w	entrainment ratio
$ZT$	figure of merit

### Subscripts

a-d	internal ejector states
B	boiler
C	cold
c	condenser
d	mixing chamber
e	evaporator
g	generator
H	hot
np	primary flow entrance
ns	secondary flow entrance
t	throat
x	pre-shock state
y	post-shock state
0	initial condition
o	stagnation property
1,2,3	different states of the system

## LIST OF ABBREVIATIONS

CFM	Cubic Feet per Minute
COP	Coefficient of Performance
CRAC	Computer Room Air Conditioner
FC	Fluoro-Carbon
HFC	Hydro-Fluoro-Carbon
IT	Information Technology
LCP	Liquid Cooled Package
NTU	Number of Transfer Units
PCM	Phase Change Material
PUE	Power Use Effectiveness
rps	rotations per second
TEC	Thermo-Electric Cooler

## SUMMARY

The purpose of this thesis is to examine possible waste heat recovery methods in data centers. Predictions indicate that in the next decade data center racks may dissipate 70kW of heat, up from the current levels of 10-15kW. Due to this increase, solutions must be found to increase the efficiency of data center cooling. This thesis will examine possible waste heat recovery technologies which will improve energy efficiency. Possible approaches include phase change materials, thermoelectrics, thermomagnetics, vapor compression cycles, absorption and adsorption systems. After a thorough evaluation of the possible waste heat engines, the use of an ejector heat pump was evaluated in detail. The principle behind an ejector heat pump is very similar to a vapor compression cycle. However, the compressor is replaced with a pump, boiler and an ejector. These three components require less moving parts and are more cost effective than a comparable compressor, despite a lower efficiency. This system will be examined under general operating conditions in a data center. The heat load is around 15-20kW and air temperatures near 85°C. A parametric study is conducted to determine the viability and cost effectiveness of this system in the data center. Included will be various environmentally friendly working fluids that satisfy the low temperature ranges found in a data center. It is determined that Ammonia presents the best option as a working fluid for this application. Using this system a Coefficient Of Performance of 1.538 at 50°C can be realized. This will result in an estimated 373,000 kW-hr saved over a year and a \$36,425 reduction in annual cost. Finally, recommendations for implementation are considered to allow for future design and testing of this viable waste heat recovery device.

# 1. INTRODUCTION

The state-of-the-art computing racks dissipate nearly 30 kW of power. Various industry benchmarking studies have been conducted to determine the distribution of power to the actual server and to the cooling equipment. Hewlett-Packard claims that 50% of the power in a data center is dedicated to cooling equipment [1]. A study group formed by the American Society of Heating Refrigeration and Air-Conditioning (ASHRAE) projects rack powers to increase even further, to nearly 70kW within the next decade, due to the introduction of ultra-dense computing architectures [2]. It is crucial that the cooling costs be contained for these very high power racks. In the current global economy conservation of energy has become a top priority. Many of the trends in data center growth have been recently presented to the United States Congress. In this report it is indicated that data centers made up 1.5% of the United States power consumption [3]. It is expected that this trend will continue and ultimately will occupy a larger percentage of the world's power consumption. In order to provide and protect the information securely, they will have to become less dependent on the current power grid.

## 1.1 Developing A More Efficient Data Center

An emerging industry index of data center energy use is the Power Use Effectiveness (PUE) - the ratio of total power into the data center to the power used by the IT equipment [4]. Since all the electrical energy going into the racks is converted to heat, recovering energy from the spent coolant stream will improve the energy efficiency of datacenters, and reduce the net power needed from the electric utility. Improving the data center's PUE in this way will also reduce operating costs and make them more environmentally friendly. It is from this perspective that there is a growing need to evaluate alternative cooling methods using waste heat for

applications in the data center. It then becomes imperative to find and evaluate the most promising methods for improving data center PUE by harvesting waste heat from the racks in the temperature range of 50°C-85°C.

## **1.2 Background Study**

A detailed literature study was carried out in two parts to allow for appropriate device selection. The first part examines waste heat recovery devices. These heat engines need to operate at low temperatures in the range of 50°C-100°C and work inside a data center. The next section examines some current state-of-the-art cooling technologies to assist in selection and operating conditions for the chosen device. The background study concludes with choosing an appropriate device for further study.

In order to identify and examine a potential waste heat recovery solution for the data center, a detailed background study of various low grade heat engines will be conducted. This will provide a basis for understanding how to effectively use low grade waste heat. Furthermore it can potentially provide a system worth further exploration. Technologies and architectures suitable for the data center will be reviewed. The technologies to be investigated include: (i) absorption refrigeration, which utilizes waste heat for compression of the working fluid within a refrigeration loop; (ii) Thermoelectric devices; (iii) as well as organic paraffin and metallic alloy PCMs for possible considerations of thermal energy storage. There will also be some consideration to vapor compression cycles. To provide for a better understanding of the current data center environment there will also be a review of existing cooling technologies. The findings will be used as guidelines for operation of the selected device.

The major goal of the study will be to investigate promising approaches for improving PUE in the data center. Then once an approach is chosen, a detailed examination and mathematical model will be created to carry out a parametric study. This will serve as a

feasibility study for the chosen solution, and provide general recommendations for operation and design of the system based on this approach.

### **1.2.1 Waste Heat Recovery Comparisons**

The various technologies examined all have the same input source, the exhaust air from the data center racks. These racks produce a range of 4-20 kW of heat currently. Future cabinets may reach as high as 100 kW and use liquid cooling. The technologies examined have been chosen based on the ability to be adapted for either a gas or liquid working fluid and have a temperature range capabilities from 50 °C to 100 °C. Furthermore, it should be noted that since this waste heat is essentially free, whether or not it is recovered, it will be produced. Thus devices with long lifetime and low initial cost become extremely attractive. Based on that assumption, the capital cost will be the driving factor for comparison, not system efficiency. Possible approaches include solid/liquid phase change materials, thermoelectrics, thermomagnetics, vapor compression cycles, absorption and adsorption systems.

#### **Phase Change Materials**

Phase Change Materials (PCMs) are latent heat storage materials. Their chemical bonds breakdown and store energy during the melting phase and when the material freezes it releases the stored heat as the bonds are reformed. A waste heat recovery system has been developed using PCMs [5]. This particular application stored the waste heat from the compressor on an air conditioner. This was then used to heat water to 80 °C for home use. For the data center application, there are two types of PCMs under consideration: paraffin waxes and salt hydrates[5].

Paraffins are of the type:  $C_nH_{2n+2}$  and the longer the hydrocarbon chain, the higher the melting point. Because of this, they come in a large range of “low heat” temperatures. Their

main draw back is the large volume change when undergoing phase changes. If space isn't a premium containers can be designed to safely handle the expansion and contain the liquid paraffin. Another key consideration is the low thermal conductivity of paraffins presents a problem when high heat transfer rates are required during the freeze cycle. However, this can be enhanced with the use of finned containers and metallic fillers [5].

Salt Hydrates consist of salt and water which forms a crystalline matrix when solid. The melting point range for Salt Hydrates varies between 15 °C and 117 °C. They are low cost and easily available. They have a sharp melting point and high thermal conductivity in the range of 0.469 W/m-K to 0.561 W/m-K. Their main drawback is upon melting they segregate and reduce the active volume for heat storage. After 1,000 cycles some salt hydrates experience a 73% reduction of heat fusion as the material settles out. This can be combated with the addition of gelled or thickened mixtures [5].

A possible application for the PCMs could be in reducing the peaks of the heat output. The PCM can store the “spikes” and release in the “valleys.” This will produce a more even heat release. In addition, as mentioned the waste heat could be captured and then discharged to a fluid for possible power generation measures. This is a possible technology to be used in series with other solutions.

### **Thermoelectrics**

Thomas Seebeck discovered a magnetic field when a closed loop was formed of two metals joined in two places with a temperature difference between the junctions. As the materials respond to the temperature difference, a current loop and resulting magnetic field is created. This principle was developed to use a temperature difference across two metals to generate

electricity. Thermoelectric devices rely on the “figure of merit” ZT for electrical performance. Equation 1 demonstrates this relationship.

$$ZT = \frac{S^2 \sigma T}{\lambda} \quad 1$$

S = Seebeck coefficient  
 $\sigma$  = electrical conductivity  
 $\lambda$  = thermal conductivity

The figure of merit is then related to the maximum conversion efficiency of the thermoelectric device as illustrated in Equation 2.

$$\eta = \frac{T_H - T_C}{T_H} \frac{\sqrt{1 + ZT} - 1}{\sqrt{1 + ZT} + \frac{T_C}{T_H}} \quad 2$$

The competing challenge in increasing the figure of merit is increasing the electrical conductivity, while decreasing the thermal conductivity. The Jet Propulsion Lab (JPL) has developed some new materials that have ZT values greater than one [3]. They discovered that the Bi<sub>2</sub>Te<sub>3</sub> alloys have the best figure of merit in the range of 100-400K. At the time of publishing (1997) the JPL had developed a ZT of just over 1 for this alloy. However, since then there has been new research which has pushed the figure of merit up towards 3 by using Czochralski-grown single crystals [6]. This study, by the *Baikov Institute of Metallurgy and Materials Science* has yielded a good advancement towards improving thermoelectric in this temperature range. However, the commercial availability still remains an issue. Current researching is focusing on nanotechnology to improve ZT at the molecular level. Work is being

done on the lattice structures of the materials to decrease the thermal conductivity [7]. However, these materials are still far away from commercial availability.

A few studies from the University of Wales Cardiff [8] challenge the idea of improving ZT. The idea of improving ZT is questioned compared to improving other economic factors. Rowe asserts that the viability of thermoelectric generation depends on the cost per Watt of electricity produced [9]. A tradeoff exists when trying to maximize the cost per Watt. For high conversion efficiency, the thermo elements should be long, however for large power output, they should be short. When balancing these two options, the economic factor should be considered. Rowe asserts when the cost of fuel is cheap, the thermoelement should be optimized for maximum power output. This, however occurs at half the attainable maximum efficiency.

Thermoelectrics could potentially be very useful in our data center applications. Since the cost of fuel is free as previously discussed, the figure of merit is not a hindrance to this solution. TECs are readily available at a conversion efficiency of about 0.6% produced by Melcore. Other arrangements of the TECs could be devised with the economic factor in mind. In addition this could be used in conjunction with PCMs to provide storage and generation.

### **Absorbtion**

The principle of absorbtion relies on the affinity of a liquid-gas mixture and its ability to absorb heat. This process is reversible and carried out with two popular gas-liquid pairs,  $\text{NH}_3\text{-H}_2\text{O}$  and  $\text{H}_2\text{O-LiBr}$ . The solution is a combination of absorbent and refrigerant. In the  $\text{H}_2\text{O-LiBr}$  solution,  $\text{H}_2\text{O}$  acts as the refrigerant and  $\text{LiBr}$  as the absorbant. This limits the system to cooling loads above  $0^\circ\text{C}$ . The Absorption systems work in a similar manner but generally use a  $\text{Li-Br}$  water solution as the working fluid. The  $\text{NH}_3\text{-H}_2\text{O}$  pair uses  $\text{NH}_3$  as the refrigerant and allows cooling below  $0^\circ\text{C}$ .

The system moves heat in the same way a vapor-compressions system behaves. However instead of a compressor, an absorber and pump are in its place as seen in Figure 1.

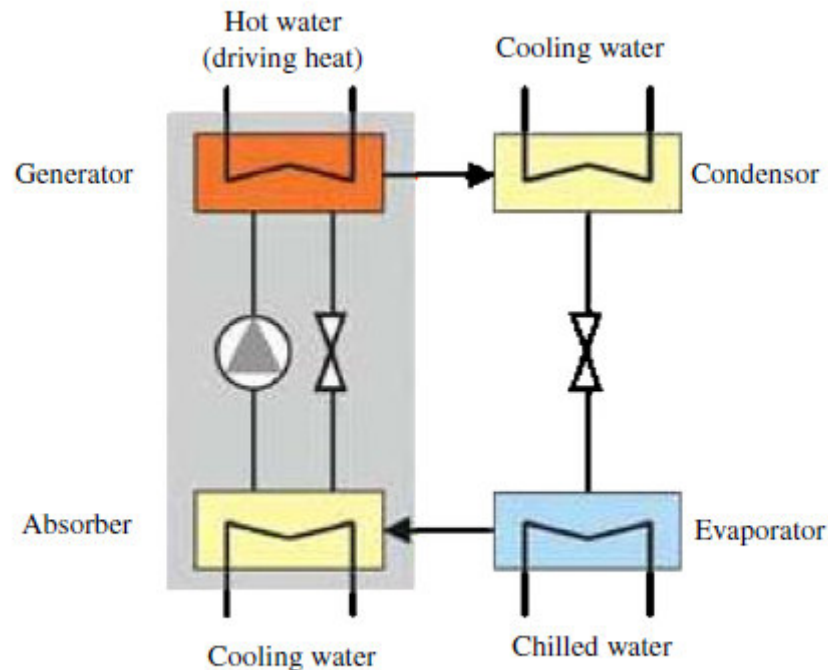


Figure 1. Absorption chiller schematic illustrating the absorber chamber [10]

The entire system is considered a reversible process. First, a pump brings the solution to a higher pressure. This solution is now heated and allows the refrigerant to separate from the absorbent. These vapors now enter the traditional vapor-compression component of an expansion valve and an evaporator. It is in the evaporator that the heat is removed and refrigeration provided. The remaining spent solution passes through a pressure-relief valve to return to the appropriate mixing pressure. The vapors from the evaporator are absorbed by the spent solution and the cycle starts again.

Absorption systems are tailored more to average ambient air temperatures and are used in some data centers today [10]. Again, there are size and initial costs similar to the adsorption

method. Comparatively, the Coefficient of Performance (COP) of an adsorption system is near 1.3-1.7 and 1.5-1.8 for absorption systems. The COP in this application is defined as the total amount of heat into the system to the amount of heat pumped out of the area. Both the adsorption and absorption systems are similar in cost and tend to be expensive in capital cost. A study conducted by the Geo-Heat center presents cost data that shows at 1000 tons of cooling the install cost of an absorption system is approximately twice as much as a comparable electric system [11].

### **Adsorbtion**

The principle of adsorbtion is concerned with the interaction of gases and solids. This is a similar system to absorbtion but uses a solid as a refrigerant instead of a liquid. In this case, the molecular interaction between the solid and the gas allow the gas to be adsorbed into the solid. The adsorbtion chamber is usually a packed bed of solid material. This allows for no moving parts and quiet operation. The primary choice for the adsorbant material is activated carbon, zeolites or silica gel. Water, methanol (ethanol) or ammonia are the most widely used adsorbates in low temperature waste heat operations. The issue with these materials involves low thermal conductivities and poor porosity characteristics.

Adsorbtion systems consist of a generator, a condenser, a pressure-relief valve and an evaporator. When the adsorbtion chamber is heated the gas is desorbed and carried through the vapor-compression cycle. In order to be absorbed the chamber needs to be cooled again. Since the adsorbant is a solid this has to take place in the same chamber. To prevent the intermittent interruption, a two bed system is used as seen in Figure 2, this adds complexity and cost.

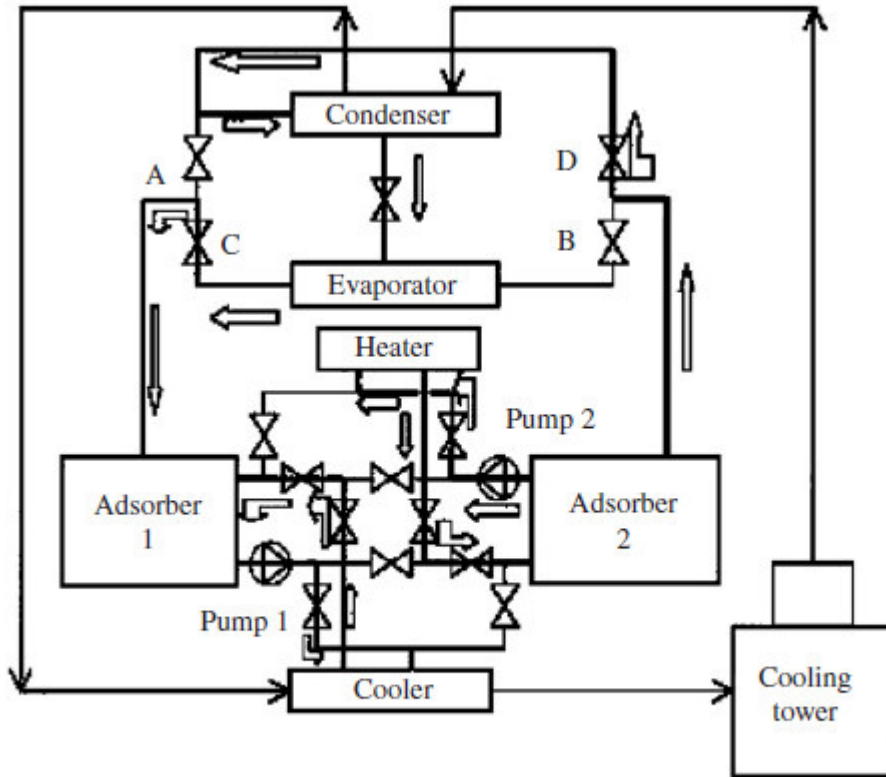


Figure 2. Adsorption refrigeration system with two bed recovery [10].

A recent study from Tokyo University details a waste heat driven three bed adsorption chiller with mass recovery [12]. The study uses 60° C to 90° C waste heat water and a cooling source of 30° C. This fits right into the goals of this work. This paper shows that there is a noticeable increase in system efficiency when mass recovery is considered. The adsorption chiller uses a silica gel/water as the adsorbant/adsorbate pair. Given the temperature requirements this system may not be feasible for generation possibilities. As temperatures rise, this may be a good way to reduce the heat in the room and discharge it out of the data center.

## Thermomagnetic Power Generation

Thermomagnetic power generation is created by taking advantage of a metal's Curie temperature. The Curie temperature is the point at which a ferromagnetic material loses its magnetic field. By choosing a material that has a Curie temperature near room temperature, the change in its ferromagnetic properties can be used with a permanent magnet to create rotational motion as depicted in Figure 3. This rotation can then be translated to electrical energy by conventional generator principles.

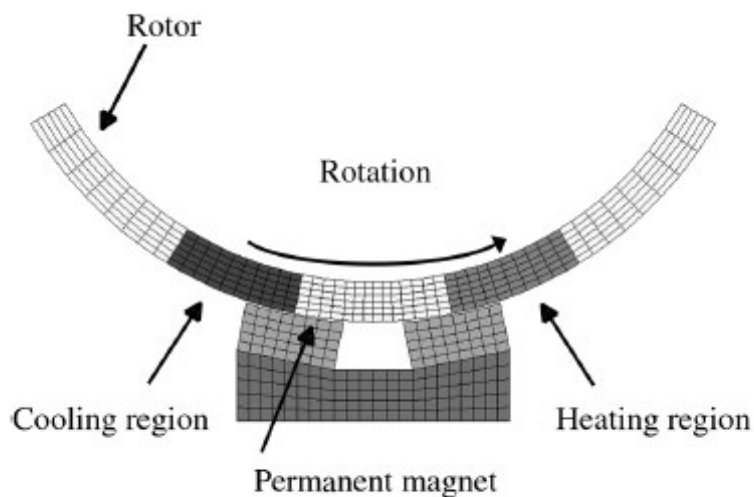


Figure 3. Schematic illustrating the thermomagnetic generator [14].

Two recent studies [13, 14] offer a different metal to consider for thermomagnetic generation. The study finds, Fe-Ni (31.5%) alloy to have the largest temperature gradient. A reduction of the eddy brake loss allows for the engine to be optimized. The rotor disk has a 400mm diameter and is made of 10 individual disks. The engine produces 14.8 W at the rotation speed of 0.76 rps. The operating conditions are a hot temperature of 90°C and a low temperature

of 11°C This technology does not seem to be commercially viable in this problem. Given that the cost of fuel is free, the capital cost of such a device will not prove feasible. The other possible options hold more promise.

These technologies all appear to have potential application to data center cooling. In order to assist in choosing the appropriate device for a detailed study, existing state of the art cooling technologies are examined.

### **1.2.2 Rack Level Cooling Technologies**

The state-of-the-art cooling technologies can be categorized into two areas by application, at the rack level and the room level. Each of these areas are beneficial to consider as the system of choice will have one or both points of application. The first group considered is the rack level applications.

Rittal is currently using a technology called Liquid Cooling Package LCP & LCP+ [15]. This high density cooling solution utilizes an air/water heat exchanger. The special horizontal airflow of the LCP represents an adaptation of this widespread cooling principle, providing cooled air uniformly throughout the complete height of the enclosure.

APC is using their technology called InfraStruXure® InRow [16]. The in-row concept closely couples cooling with the heat load, preventing exhaust air recirculation to sensitive IT equipment. Heat rejection for the chilled water InRow can be handled through an existing chilled water system or APC supplied chiller.

IBM is using Cool Blue: Rear Door Heat Exchanger. This device hinges to the back of a rack, with a hose installed in the floor that goes up the door. Sealed tubes filled with chilled water remove up to 55% of the heat generated in a fully populated rack. This rear door heat

exchanger allows for the removal up to 50,000 BTU or 15.5 kW of heat generated by a full server rack [17].

The rack level cooling devices are summarized in Table 1 below. The specifications will be used as guidelines for operation of the device under study.

Table 1. State-of-the-art comparisons for rack level cooling.

	<b>APC</b>	<b>Rittal</b>	<b>IBM</b>
<b>Size [m]</b>	H: 1.99 D: 0.29 W:1.07	H: 2.03 D: 0.91 W: 1.02	H: 1.87 D: 0.10 W: 0.66
<b>Cooling Fluid</b>	Water	Water	Water
<b>Water Inlet Temperature [°C]</b>	7.0	1-30	18
<b>Cooling Capacity [kW]</b>	70 (35 two sides)	2-30	12-15
<b>Air Flow Rate [m<sup>3</sup>/min]</b>	82.1	39.9	N/A
<b>Water Flow Rate Max [L/min]</b>	50.34	15	30.28-37.85

This survey of state-of-the-art technologies highlights three different cooling solutions that rely on cooling units in the same row as the server racks. These units are the most efficient methods of cooling and are in use in the current data center environment. The current availability and proven use of these heat exchangers presents an attractive component to a possible design solution.

### 1.3 Device Selection

Of the approaches examined, the absorption/adsorption systems were direct cooling methods, rather than utilizing waste heat energy for power or cooling energy. The method of using absorption/adsorption systems would provide a way to lower the cooling load and more efficiently cool the data center but not reduce the power consumption into the data center. The phase change materials, thermoelectric devices and the thermomagnetic present ways to generate or store electrical energy, but their efficiencies were too low with too large of an initial cost. It was concluded that providing cooling would be more effective than generating electrical power from the waste heat. However, for the absorption/adsorption systems the initial cost is large and then miniaturization presents challenges.

These ideas come together very well in the use of an ejector based refrigeration system. The general principle is that the traditional vapor-compression cycle is modified to exchange the compressor for a pump, boiler and ejector. Furthermore, this system would allow for a reduction in the number of CRACs in the data center. According to an analytical model of data center efficiency from IBM the CRAC fans account for 27% of the cooling energy [18]. A detailed explanation is provided below. This particular system will use the waste heat at the rack level to run a refrigeration system in the data center.

## 2. EJECTOR HEAT PUMP METHODS

The ejector heat pump works in a similar fashion to a conventional vapor compression refrigeration cycle. However, instead of a mechanical compression device, an ejector is used to compress the refrigerant vapor to the condenser pressure. The study by CT Hsu at the University of Tennessee examines this system closely [19]. The schematic design is seen below in Figure 4.

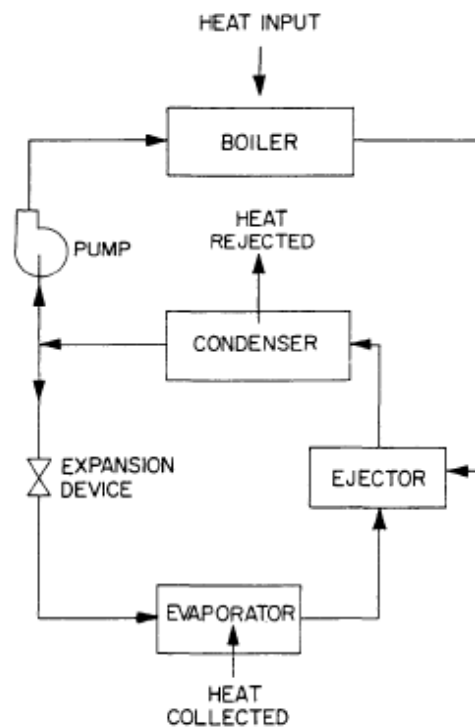


Figure 4. Ejector Heat Pump schematic [19]

This system could use the waste heat to drive a boiler if an appropriate working fluid is chosen. Hsu examines R113 and R11, yielding a COP around 0.3 for a boiler temperature of

473 K. The COP is defined as the total heat input into the evaporator divided by the heat input to the boiler. The main challenges are in ejector design and tailoring the system to the data center layout.

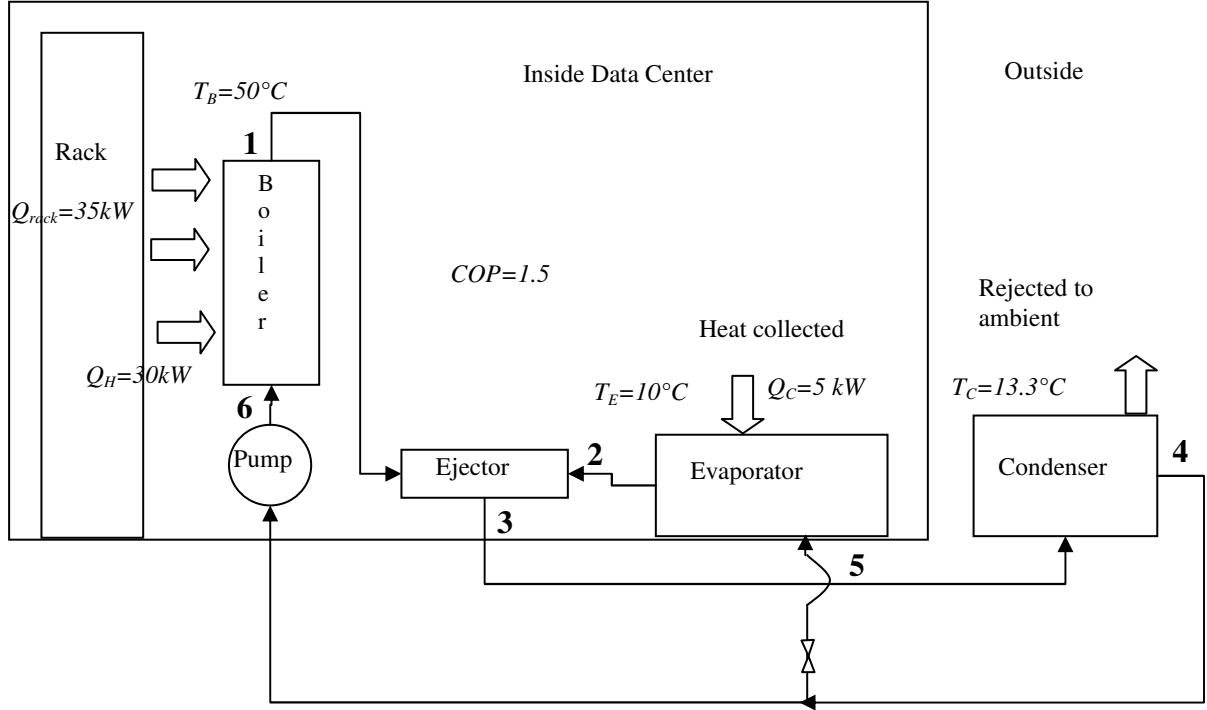


Figure 5. Proposed data center application

## 2.1 Pump and Boiler Model

The Ejector Heat pump departs from a traditional vapor compression cycle at the compressor component. The traditional compressor is replaced with a pump, boiler and ejector components. The pump work is modeled using constant specific volume using Equation 3, as seen below.

$$W_{pump} = \dot{m}_g \cdot v_4 \cdot (P_6 - P_4) \quad 3$$

The boiler is modeled as a basic shell and tube heat exchanger. Performing an energy balance over the exchanger yields Equation 4 to model the boiler.

$$Q_{boiler} = m_b (h_1 - h_6) \quad 4$$

After the pump raises the working fluid to the saturation pressure, the heat input,  $Q_{boiler}$ , changes the phase from liquid to vapor as it prepares to enter the Ejector component.

## 2.2 Ejector Model

The idea of an ejector has been around for nearly a century [19]. The basic idea is to entrain a secondary fluid to create compression of that fluid. Parts of the process, specifically the mixing and compression is done at supersonic speeds and relies on choked flow. Both flows are modeled as ideal gases and enter the ejector with a quality of 1. Figure 6 shows the important sections of an ejector.

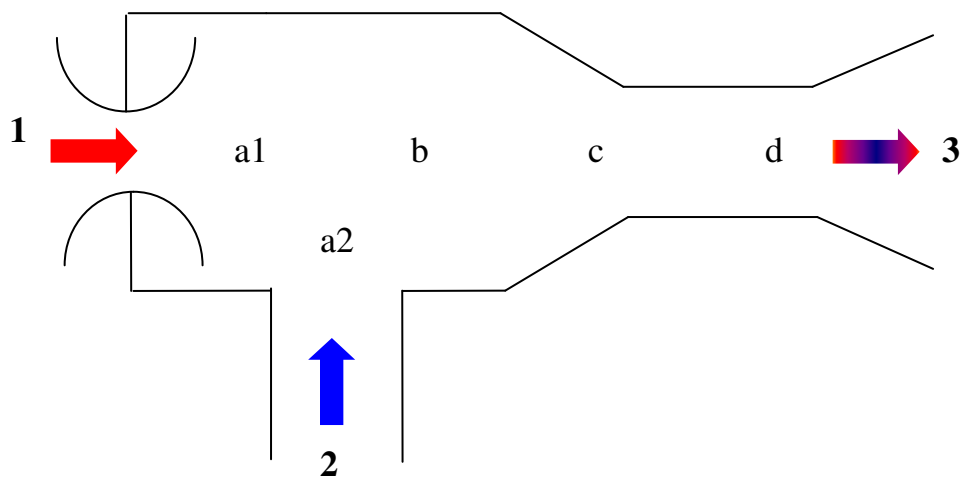


Figure 6. Ejector schematic with state locations identified.

At State 1, the high pressure, high energy motive stream enters the ejector. State 2 is where the secondary, low pressure stream enters the ejector. At both points, the temperature and pressure are known. The points marked a1 and a2 are the property states after the stream has passed through the ejector nozzles. The pressure in this region is set such that the flow through state 2 is sonic. With this condition, the flow is choked and maximum flow rate is achieved

through entry 2. Since the pressure required to achieve this condition is less than the critical pressure of flow through entry 1, the flow through that entry will be supersonic, choked and also at a maximum flow rate. The critical pressure is determined by Equation 5.

$$P_{critical} = \frac{P}{\left(1 + \left(\frac{k-1}{2}\right) \cdot M^2\right)^{\frac{k}{k-1}}} \quad 5$$

To find the critical pressure for the secondary flow, Equation 5 is used with  $P = P_e, M = 1$ . This critical pressure will be the constant mixing pressure in the region for mixing at State b.

With compressible flows it is easier to deal with reference states known as Stagnation State Properties. This gives a relationship between velocity and specific enthalpy for a given stagnation state as seen by Equation 6.

$$h_0 = h + \frac{V^2}{2} \quad 6$$

The stagnation states for the ejector are represented by the inlet and outlet numbers in Figure 6. As the properties change, the relationship in Equation 6 can be used to find the velocity at each point. The nozzle at state 1 is assumed to have a particular isentropic efficiency and given the critical mixing pressure from Equation 5 the specific enthalpy,  $h_b$  can be determined [20]. With this information and the enthalpy at Stagnation State 1,  $V_{a1}$  can be determined from Equation 7.

$$V_{a1} = \sqrt{2 \cdot (h_1 - h_{a1})} \quad 7$$

For an ideal gas, the speed of sound obtained with isentropic expansion from local stagnation conditions is found by Equation 8.

$$c = \sqrt{k \cdot \bar{R} \cdot T_{stag}} \quad 8$$

The Mach number,  $M^*$  is then defined by Equation 9.

$$M^* = \frac{V}{c} \quad 9$$

Once  $V_{a1}$  is known, Equations 8 and 9 can be used to determine  $M_{a1}^*$ . The same method can be applied to Stagnation State 2 to find  $V_{a2}$  and  $M_{a2}^*$ . However by the definition of critical pressure,  $M_{a2}^*$  should be very close to 1, indicating sonic flow.

Once the specific Mach numbers are known, the mixing results are found using Keenan's[21] relationship for mixing of two streams at constant pressure as seen in Equation 10

$$M_b^* = \frac{M_{a1}^* + w \cdot M_{a2}^* \cdot \sqrt{\tau}}{\sqrt{((1 + w \cdot \tau) \cdot (1 + w))}} \quad 10$$

Where  $M^*$  is the particular state's velocity divided by the velocity of sound obtained with isentropic expansion from local stagnation conditions. In Equation 10,  $\tau$  is defined as the temperature of the secondary stream divided by the temperature of the motive stream.

The entrainment rate is defined as variable  $w$  and is the ratio of secondary stream flow rate to the motive stream as seen in Equation 11.

$$w = \frac{\dot{m}_e}{\dot{m}_b} \quad 11$$

In this particular case it is the mass flow rate of the evaporator,  $\dot{m}_e$  per flow rate of the boiler,  $\dot{m}_b$ . The goal of this study is to maximize  $w$  given the temperatures of the boiler and evaporator and the condenser pressure.

An energy balance is performed on the ejector in Equation 12 and the energy balance in terms of  $w$  is displayed in Equation 13.

$$\begin{aligned} \dot{m}_b h_1 + \dot{m}_e h_2 &= (\dot{m}_b + \dot{m}_e) h_3 \\ h_1 + \frac{\dot{m}_e}{\dot{m}_b} h_2 &= \frac{(\dot{m}_b + \dot{m}_e)}{\dot{m}_b} h_3 \end{aligned} \quad 12$$

$$h_1 + w h_2 = (1 + w) h_3 \quad 13$$

The mixed Mach number at location b is found using Equation 10 and then converted to velocity  $V_b$  at the location. Using State 3 as the stagnation state for location b, the total energy can be found from Equation 14.

$$h_3 = h_b + \frac{V_b^2}{2} \quad 14$$

After the streams are mixed at State b, the flow is sent through a divergent nozzle with an assumed isentropic efficiency. This causes the flow to enter State c at super sonic velocity. The specific enthalpy,  $h_3$  can be determined by the nozzle conditions and the velocity,  $V_c$  can be solved using Equation 6 with  $h_3$  as the Stagnation state.

$$V_c = \sqrt{2 \cdot (h_3 - h_c)} \quad 15$$

If the flow is supersonic as it enters the constant area throat, a shock wave occurs between State c and State d. This normal shock comes with an increase in entropy and a jump in pressure before and after the shock. Fanno and Rayleigh lines are used to derive the normal shock equations. These equations represent the fluid properties and heat transfer considerations respectively. The energy across the shock must balance and these two lines intersect at two specific locations and represent the change in entropy give a particular Mach number. From

these energy balances, Equations 16-20 are derived. The shock relations are demonstrated in the following equations.

The pre shock Mach number is determined from the velocity at state c.

$$M_x = \frac{V_c}{c} \quad 16$$

Using normal shock relations, the post-shock Mach number,  $M_y$  is found by Equation 17.

$$M_y^2 = \frac{M_x^2 + \left(\frac{2}{k-1}\right)}{\left(2 \cdot \frac{k}{k-1}\right) \cdot M_x^2 - 1} \quad 17$$

There is a similar relationship for the pre-shock pressure,  $P_x$  and post-shock pressure,  $P_y$ . Equations 18 and 19 are solved to determine the pressures.

$$\frac{P_x}{P_{critical}} = \left( \left( \frac{k-1}{2} \right) \cdot M_x^2 + 1 \right)^{\frac{k}{k-1}} \quad 18$$

$$\frac{P_y}{P_x} = \left( \frac{1+k \cdot M_x^2}{1+k \cdot M_y^2} \right) \quad 19$$

These pre and post shock pressures relate to the pressures at state c and state d respectively. After passing through the constant area throat section from c to d, the flow is expanded through a diffuser with a given isentropic efficiency to the condenser pressure. This relationship is seen in Equation 20.

$$\frac{P_c}{P_y} = \left( \left( \frac{k-1}{2} \right) \cdot M_y^2 + 1 \right)^{\frac{k}{k-1}} \quad 20$$

The design condition at State 3 is that the pressure must match that of the condenser. This condition is specified in Equation 20. With Equations 13 and 14, the specific enthalpy at State b,  $h_b$  and total enthalpy at  $h_3$  can be determined and  $w$  solved iteratively.



Table 2. Vapor Ejector processes by state.

<b>State</b>	<b>Process</b>
1-a1	Expansion through converging diverging nozzle, $V_{a1}$ is supersonic
2-a2	Isentropic convergence through nozzle, $V_{a2}$ is sonic and $P=P_{critical}$
b	Constant pressure mixing occurs at $P=P_{critical}$
b-c	Convergence through nozzle, $V_c$ is supersonic
c-d	Normal shock through constant area throat section. Modeled with Fanno-Rayleigh lines.
d-3	Expansion through diffuser to Condenser pressure.

### 2.3 Ejector Area and Size Considerations

In developing the ejector model, the area of the various regions is an important area of discussion. Previous papers deal with ejector geometry for explicit operating conditions [21, 22]. The geometry and performance are highly dependent on one set of optimal conditions. Any variation from the optimal conditions drastically reduces the ejector performance. The important areas to consider are indicated in the figure below designated by A with a subscript.



$A_{np}$  indicates the cross sectional area of the primary flow and  $A_{ns}$  the area of the secondary flow. Their relationship is defined in Equation 23.

$$\frac{A_{ns}}{A_{np}} = \left(\frac{P_1}{P_2}\right)^{1/k} \cdot \left( \frac{\sqrt{\left(1 - \left(\frac{P_{critical}}{P_1}\right)^{\frac{k-1}{k}}\right)}}{\sqrt{\left(1 - \left(\frac{P_{critical}}{P_2}\right)^{\frac{k-1}{k}}\right)}} \cdot w \cdot \sqrt{\left(\frac{T_2}{T_1}\right)} \right) \quad 23$$

These two are based on their initial pressure and the critical mixing pressure. Generally  $A_{ns}$  is larger than  $A_{np}$  in order to allow the secondary fluid to be pulled into the ejector. Finally  $A_d$  is the mixing chamber and relates to  $A_t$ , the throat area as seen in Equation 24.

$$\frac{A_t}{A_d} = \left(\frac{P_3}{P_1}\right) \cdot \sqrt{\frac{1}{(1+w) \cdot \left(1 + w \cdot \frac{T_2}{T_1}\right)}} \cdot \left( \frac{\left(\frac{P_{critical}}{P_3}\right)^{1/k} \cdot \sqrt{\left(1 - \left(\frac{P_{critical}}{P_3}\right)^{\frac{k-1}{k}}\right)}}{\left(\left(\frac{2}{k+1}\right)^{\frac{1}{k-1}} \cdot \sqrt{\left(1 - \left(\frac{2}{k+1}\right)\right)}\right)} \right) \quad 24$$

After examining the previous studies there are two regions to fix the area. Region I is the relationship between  $A_t$ ,  $A_{ns}$ , and  $A_{np}$  and Region II is the relationship between  $A_t$  and  $A_d$ .

The study conducted by Alexis [22] discusses the optimal geometries based on initial temperature of the boiler/generator, condenser and evaporator. Thus the areas change with a variation of those parameters. Region I and II are free to adjust to the optimal areas and thus give an ideal COP for each temperature.

The Hsu study addresses the issue of constant area in its Off Design Study. However, the Hsu model relies on constant area mixing where the current model relies on constant pressure mixing. The constant pressure mixing model is more common and relies on choked flow to achieve maximum flow rates. In the Hsu paper, the nozzle openings for the primary and secondary flows are not considered; only Region II is considered. This does raise the idea of keeping one of the ejector parameters constant and evaluating the change in performance. However, this is not the best model for the data center application because the geometries will be completely fixed as the ejector will be a ridged component of the system.

The study by El-Dessouky [23] addresses the nozzle openings and appropriate geometries for constant pressure mixing. The focus of the current study is Region I. Several of the other equations also match the model under development; thus, many of the previous area considerations are derived from this study. However, once again this paper discusses the design in terms of optimal operating conditions and not fixed geometries that would be present in a data center application.

The conclusion from these papers is that the models currently in use can only effectively fix one of the regions considered. Since Region I dictates the speed at which the fluid enters the ejector this is an important area to focus on. Therefore as this study is conducted, the area relations are fixed for Region I and  $A_d$  is left to find its optimum dimension.

The size of the ejector is generally defined as its length and largest diameter. The diameter of the largest section,  $A_{ns}$  is determined by Equation 25 and is referred to as the ejector diameter.

$$EjectorDiameter = \sqrt{\frac{4 \cdot A_{ns}}{\pi}} \quad 25$$

The throat diameter is defined in a similar way in Equation 26.

$$D_t = \sqrt{4 \cdot \frac{A_t}{\pi}} \quad 26$$

The length is determined based on the recommendations from ASHRAE [24]:

- a. The mixing section will be 6–10 throat diameters long, with an average value of 7.
- b. The constant-area throat section is typically 3–5 throat diameters long to accommodate the shock pattern and its axial movement under load.
- c. The subsonic diffuser has an axial length of 4–12 throat diameters is found in practice.

From these recommendations, a maximum and minimum length will be determined to give the maximum range of the ejector. These length will be based on Equation 27, displayed below.

$$\begin{aligned} EjectorLength_{\max} &= 27D_t \\ EjectorLength_{\min} &= 13D_t \end{aligned} \quad 27$$

## 2.4 Evaporator, Condenser and Throttle Models

The condenser is modeled the same as in a typical vapor compression system. Similar to the boiler, an idealized, reduced energy balance is used and seen below in Equation 28.

$$Q_{evaporator} = \dot{m}_e \cdot (h_2 - h_5) \quad 28$$

After the fluid has passed through the ejector, it exits at the condenser pressure. For this system model, the ideal conditions of a typical condenser are used. After reducing the energy balance, this yields Equation 29, used to model the condenser.

$$Q_{condenser} = (\dot{m}_g + \dot{m}_e) \cdot (h_3 - h_4) \quad 29$$

As the working fluid exits the condenser, part of the stream is split to return to the evaporator, and the other part heads to the pump-boiler components. In order to reduce the pressure from the condenser to match the evaporator, an ideal throttling process is modeled as Equation 30.

$$h_5 = h_4 \quad 30$$

## 2.5 Performance Metrics

The most common form of measuring refrigeration systems is in the form of Coefficient of Performance (COP). In the proposed data center solution, the goal is to remove the waste heat and use it to provide cooling. This will ultimately relate to a reduction in electrical power and increase the data center PUE. It is for this reason, that the COP is defined as displayed in Equation 31.

$$COP_{ejector} = \frac{Q_{boiler} + Q_{evaporator}}{Q_{boiler}} \quad 31$$

The COP of this system will always be 1 or above, indicating that even in the case the ejector doesn't function, the heat going into the boiler will be rejected in much the same way as a rear door heat exchanger. Since this system is waste heat driven, the only power input is into the pump and is defined in Equation 32, where  $v_4$  is the specific volume of the fluid as it passes through State 4.

$$W_{pump,ejector} = \dot{m}_g \cdot v_4 \cdot (P_6 - P_4) \quad 32$$

Since the goal of this design study is to reduce the electrical input into data center cooling, the pump work is a very important design consideration and will be used to compare this Ejector Heat Pump to a traditional Vapor Compression Cycle.

## 2.6 Ejector Model Validation

To verify the accuracy of this model, predictions from the ejector model are compared to published data with the same working fluid. After the validation, the entire Ejector Heat Pump model is used for parametric studies. To accurately verify the ejector model, the results are compared to two previous studies conducted by Kouremenos and Alexis. The ejector model verification test uses water as the working fluid, and adjusts the temperatures and pressures to match the specific studies.

The first comparison is in the study conducted by Kouremenos.[20] The data should match the presented trends in Figure 7. For  $P_b= 800$  kPa,  $T_e=283$ K and  $T_c=323$ K the comparison is presented in Figure 9.

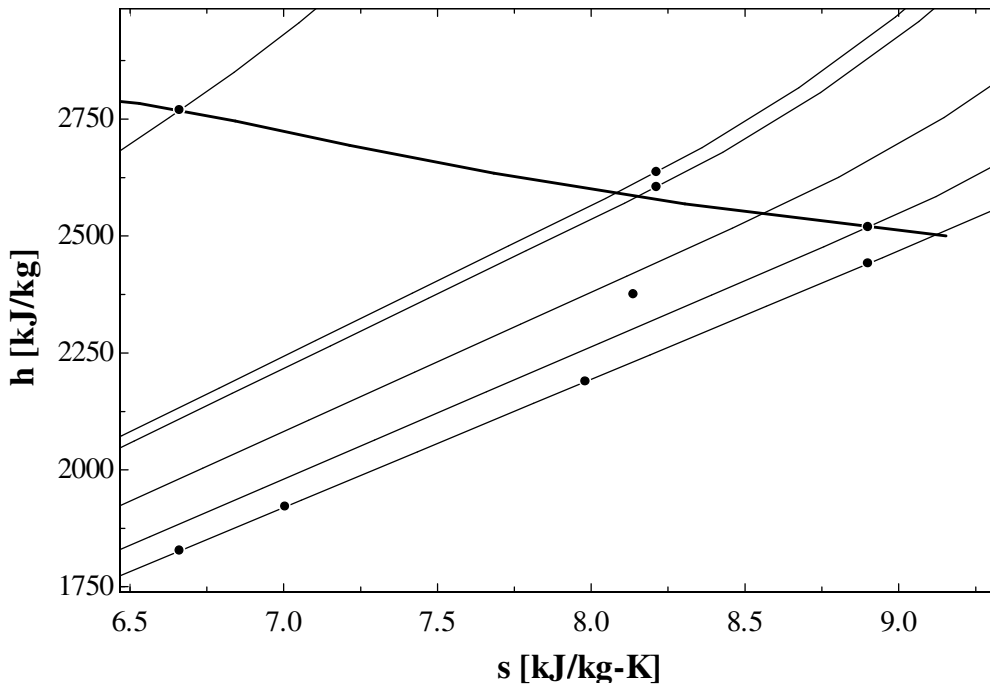


Figure 9. Ejector Model verification, each point represents the state as described in Table 3.

Figure 9 demonstrates the correct trends similar to Figure 7 in the Ejector Model section. The appropriate mixing occurs and the energy balances. This is evident by seeing that the

mixing point as described in Table 2 is on the same pressure contour and located between the primary and secondary flow enthalpies near an enthalpy of 8 kJ/kg-K.

The second comparison is with the given entrainment rate as presented by Alexis. The Alexis paper presents maximum entrainment rates for a fixed generator pressure, three different condenser temperatures and a range of evaporator temperatures. The generator is fixed at 800 kPa, the three condenser temperatures are 323 K, 318 K, and 313 K with an evaporator range of 277 K-283 K. The specific heat value is 1.3 KJ/kg-K and the diffuser is set to 100% efficient to agree with the data in the study. Figure 6 shows the comparison.

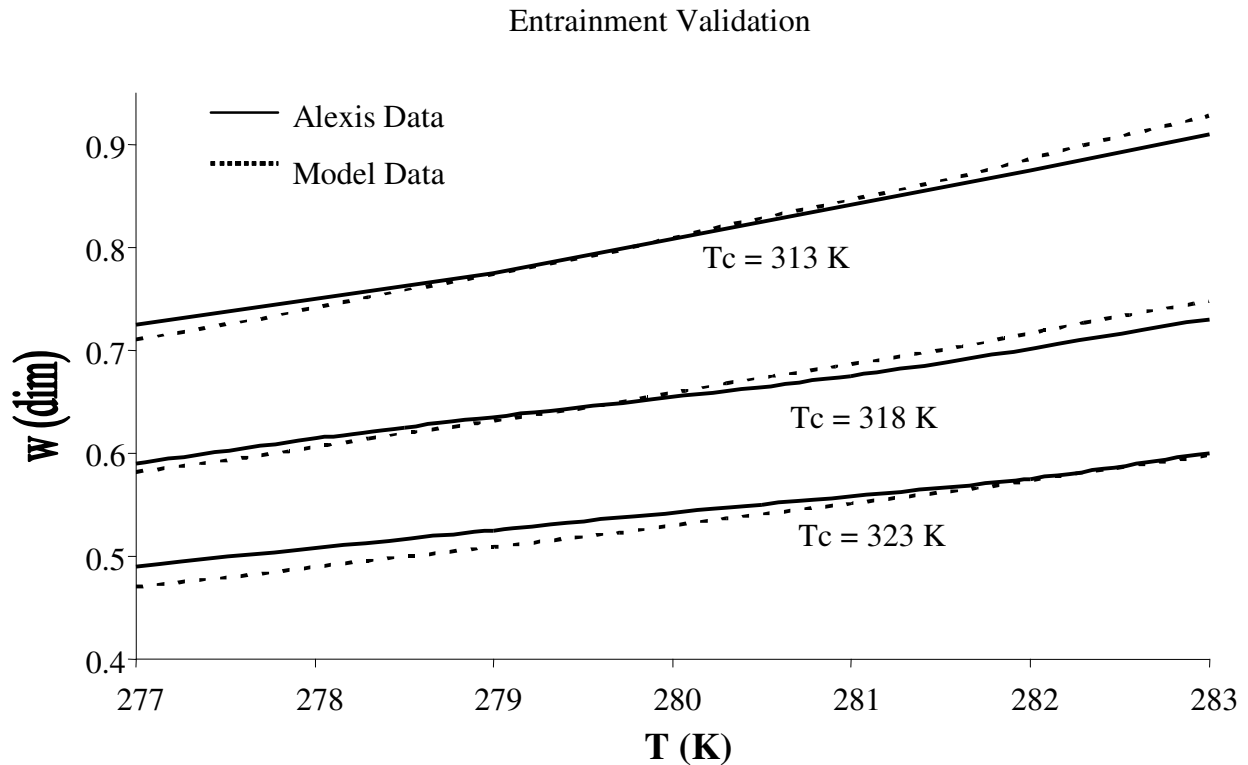


Figure 10. Entrainment validation comparing the model data with the published data.

There is good agreement between the model and the published data. There are a few considerations that explain the small differences. The specific heat ratio affects the model results, as well as the diffuser efficiency. An increase in the specific heat ratios moves the entrainment value higher and a lower efficiency reduces the maximum entrainment rate.

Based on the two comparisons of the model with published data, it appears the ejector model is good to complete the study. The energy balances well and exhibits similar trends to the expected Mollier diagram as previously discussed. Furthermore the entrainment rates closely match the published data.

In order to validate the entire ejector heat pump model, comparison is made to the Hsu paper using the working fluid of R11. In the study conducted by Oak Ridge National Laboratory, Hsu presents a large scale ejector system using various hydrocarbons. That model is not entirely applicable to the data center environment, but provides useful information for an comparison. This study will not consider R11 except for the purpose of validating the model. The initial conditions presented in the Hsu paper are presented below in Table 4.

Table 3. Initial conditions for R11 model validation with the Hsu study

$T_g$	366 K
$T_e$	283K
$T_c$	316 K
$\eta_n$	0.97
$\eta_d$	0.75

Using the same inputs into the model underdevelopment yields the following T-s diagram presented in Figure 11 and the performance results presented in Table 3.

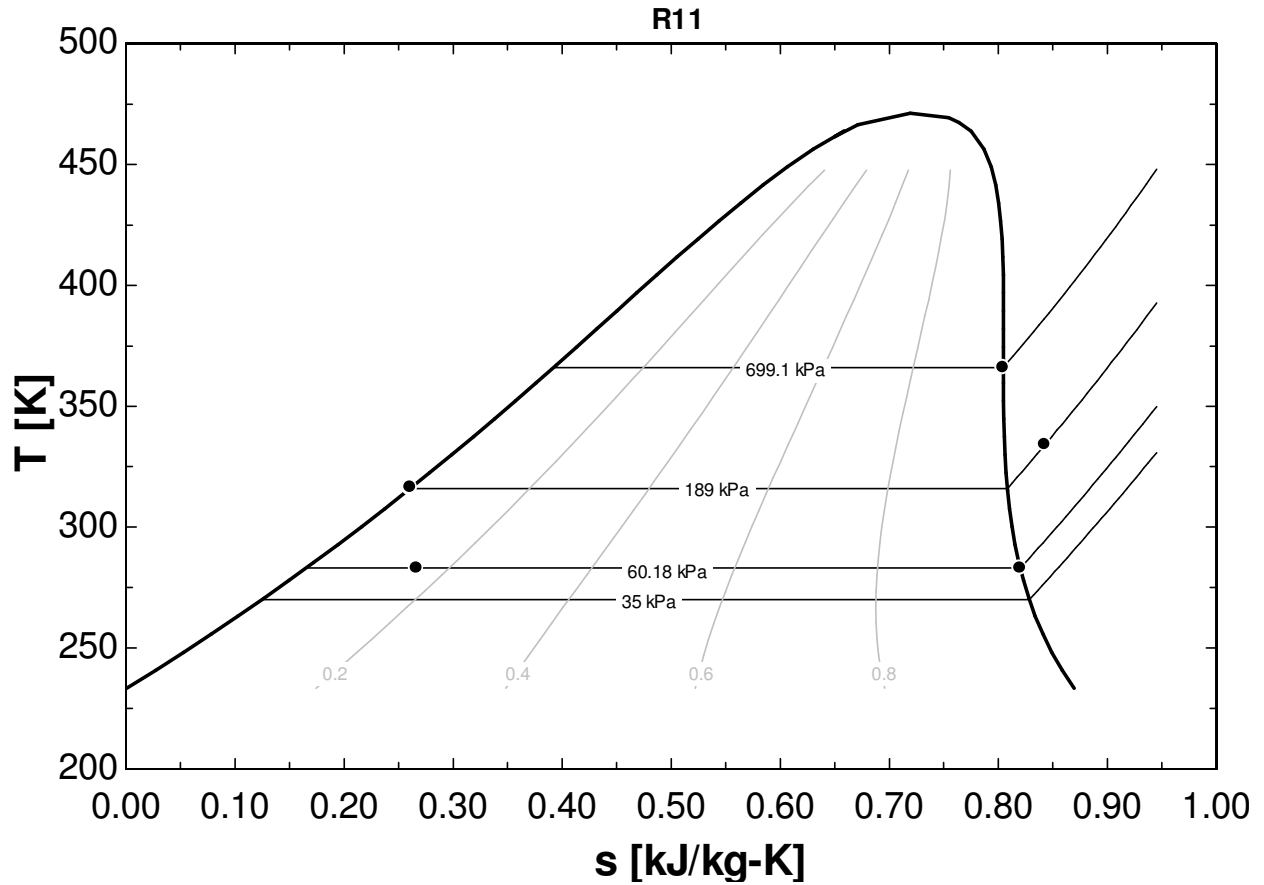


Figure 11. R11 Comparison results

Table 4. R11 Model Comparisons

	<b>Current Study</b>	<b>Hsu</b>
<b>COP</b>	0.34	0.307
<b>w</b>	0.43	0.38

Figure 11 presents the T-s diagram for the model is being validated. The location of the states matches the expected trends from Hsu. Furthermore, a comparison of the COP and

entrainment rate,  $w$  demonstrates close agreement. It appears that the present model has a slightly higher COP and entrainment rate. The present model uses a critical mixing pressure that is below the evaporator pressure, allowing for choked flow in both the primary and secondary nozzles. This slightly increases the entrainment rate. Since the entrainment rate is related to the amount of heat removed through the evaporator, an increase in entrainment rate will also raise the COP. This explains why the COP is slightly higher. In Table 5, the detailed information for each state is available.

Table 5. Detailed comparison data for each state of the ejector heat pump cycle.

State	Temperature (K)		Pressure (kPa)		Enthalpy (kJ/kg)		Entropy (kJ/kg-K)	
	Present Study	Hsu	Present Study	Hsu	Present Study	Hsu	Present Study	Hsu
1	366.00	366.00	699.10	706.70	267.30	267.00	0.8044	0.8040
2	283.00	283.00	60.18	60.50	227.90	228.00	0.8200	0.8207
3	334.20	335.80	189.40	192.30	255.50	257.00	0.8428	0.8458
4	316.00	316.30	189.40	192.30	71.21	71.60	0.2607	0.2638
5	283.00	283.00	60.18	60.50	71.21	71.60	0.2665	0.2679
6	316.50	383.72	699.10	706.70	71.62	72.00	0.2607	0.2638

Upon careful examination of the states it can be seen that the two models generally agree for the same initial conditions. This further demonstrates the validity of the model. Figure 11 provides the general trend for the other working fluids will as well.

## 2.7 Working Fluid Options

For this study, five working fluids have been considered. For the data center application there are several factors to consider. The first concern is the environmental impact and future

allowability of the particular fluid. Many refrigerants are being phased out due to global warming and ozone potential. It is for this reason that the Hsu study using R11 is now outdated. Next is the ability to operate in the 50 °C to 100 °C. Originally these ejector systems were built to run with steam, which presents a challenge given the current data center applications. Since the system is closed, there is no expected contact with the electronics, this allows for working fluids that may not be completely inert. The last consideration is that of cost. Based on these considerations, the following working fluids have been chosen: R134a, R141b, Ammonia, FC87 and FC72. Each of these fluids have some variance from the ideal working fluid, but they do present readily available options and are appropriate for this study. Each fluid under consideration is presented with its T-s diagram and the state locations from the model. Each fluid is examined and discussed based on its comparison to Figure 11, the validated R11 model. Of the refrigerants under study they are in three groups: Ammonia, Hydro Fluorocarbons (HFC) and FC's.

In the case of Ammonia, the T-s diagram, below in Figure 12 matches very well with the R11 validation and the code operates well with the model under consideration. Ammonia presents a severe risk to humans in high concentrations, but its release of a strong odor make it easily identifiable and safe to use in refrigerant applications. Ammonia presents no ozone risk and is environmentally friendly [25]. There are current systems in place using ammonia.

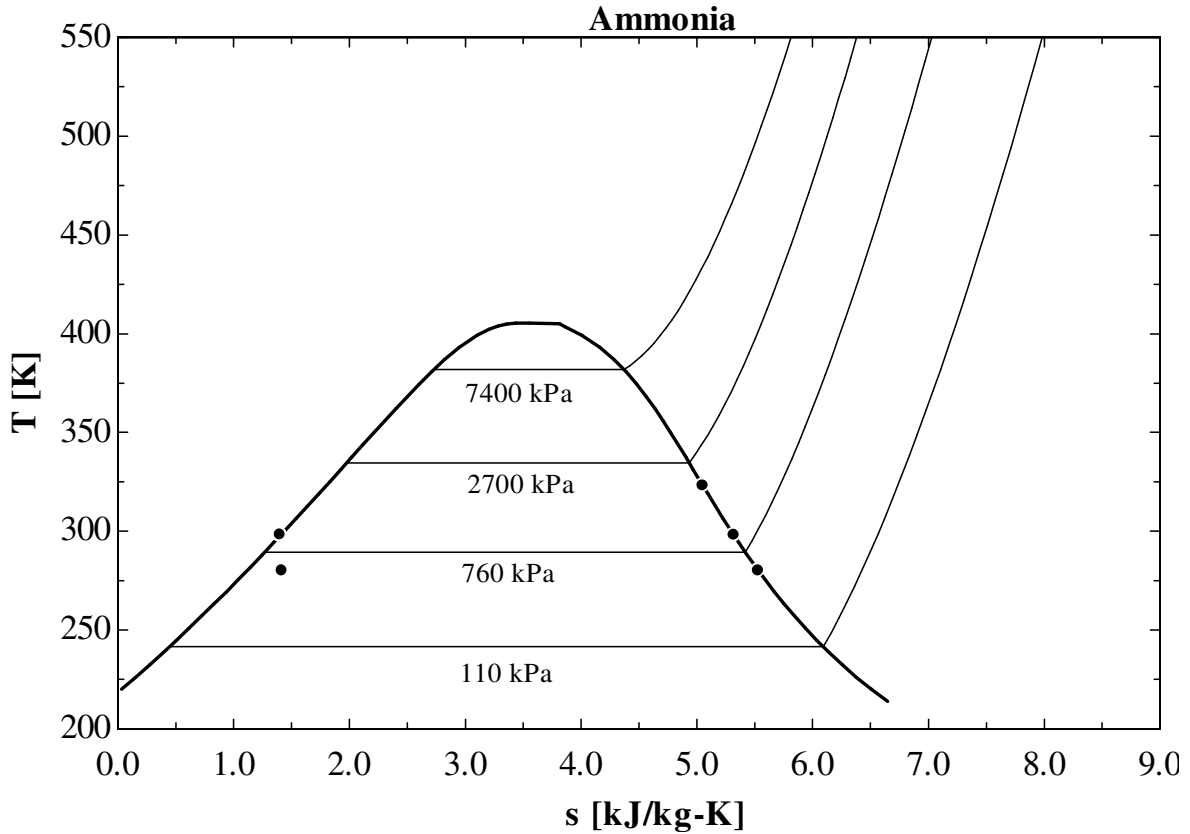


Figure 12. T-s diagram for Ammonia, highlighting the similar trends and state locations to R11

The HFC group or commonly referred to as refrigerant and an identifying number, such as R134a has a slightly steeper slope on the T-s diagram seen in Figure 13. The outlet point (State 3) actually has slightly higher entropy than the lower point (state 2) however there are no second law violations. Various types of HFC's have been banned from the Montréal Protocol and present some ozone risks. However they are extremely stable and efficient. If used responsibly, various common and new HFC's are viable options [26]. For the model study, R134a is examined.

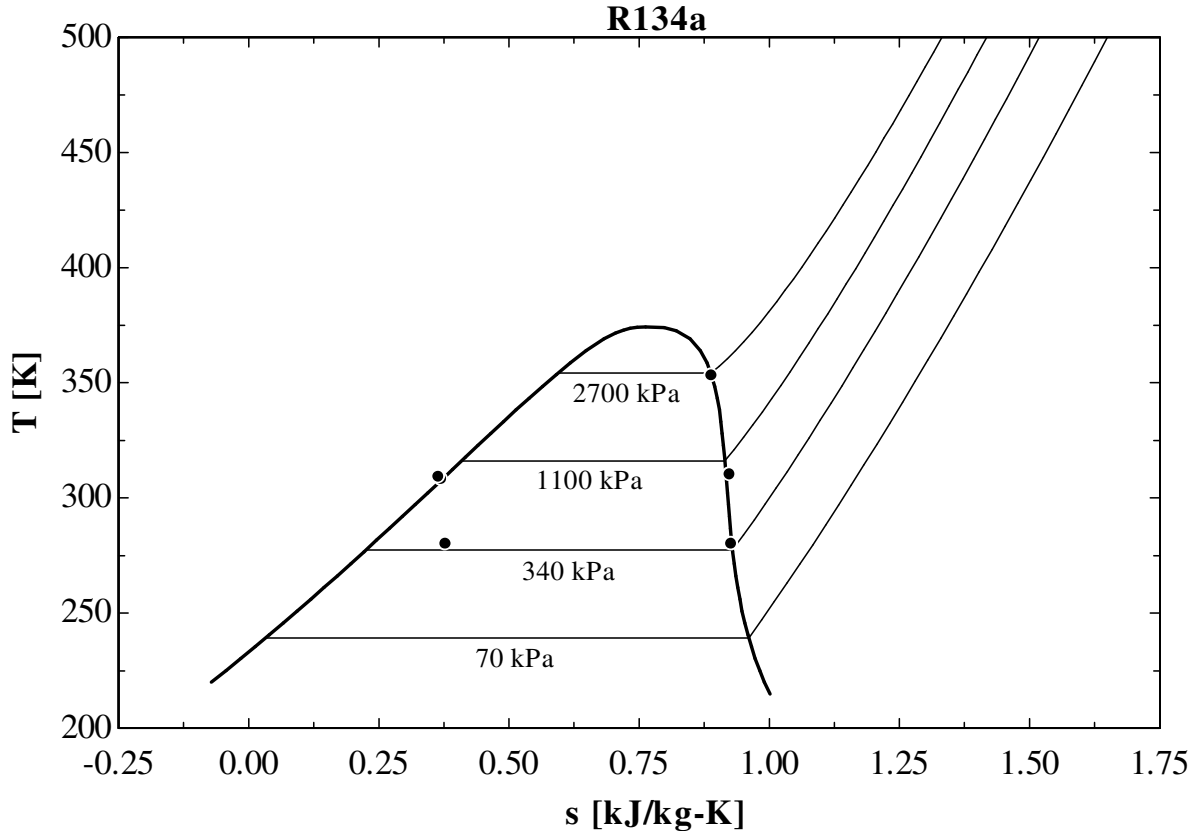


Figure 13. T-s diagram for R134a, highlighting the similar trends and state locations to R11

The last group is FC87 and FC72 or 3M's Fluorinert presented in Figure 14. These fluids have been developed for direct contact with electronics and are the least reactive and most stable. However, the FC group has the largest difference in behavior. The slope of the line is actually inverse of the previous T-s diagrams. This creates an interesting scenario with regards to the entropy of the inlet states. In this case  $s_2 > s_1$  which is opposite of the previous cases. Again, there is no second law violation, but there may be some complications in the models. The model returns an entrainment rate greater than one which causes an unbalance in the conservation of mass. A drawback is that these fluids are much more expensive than the previous fluids under consideration.

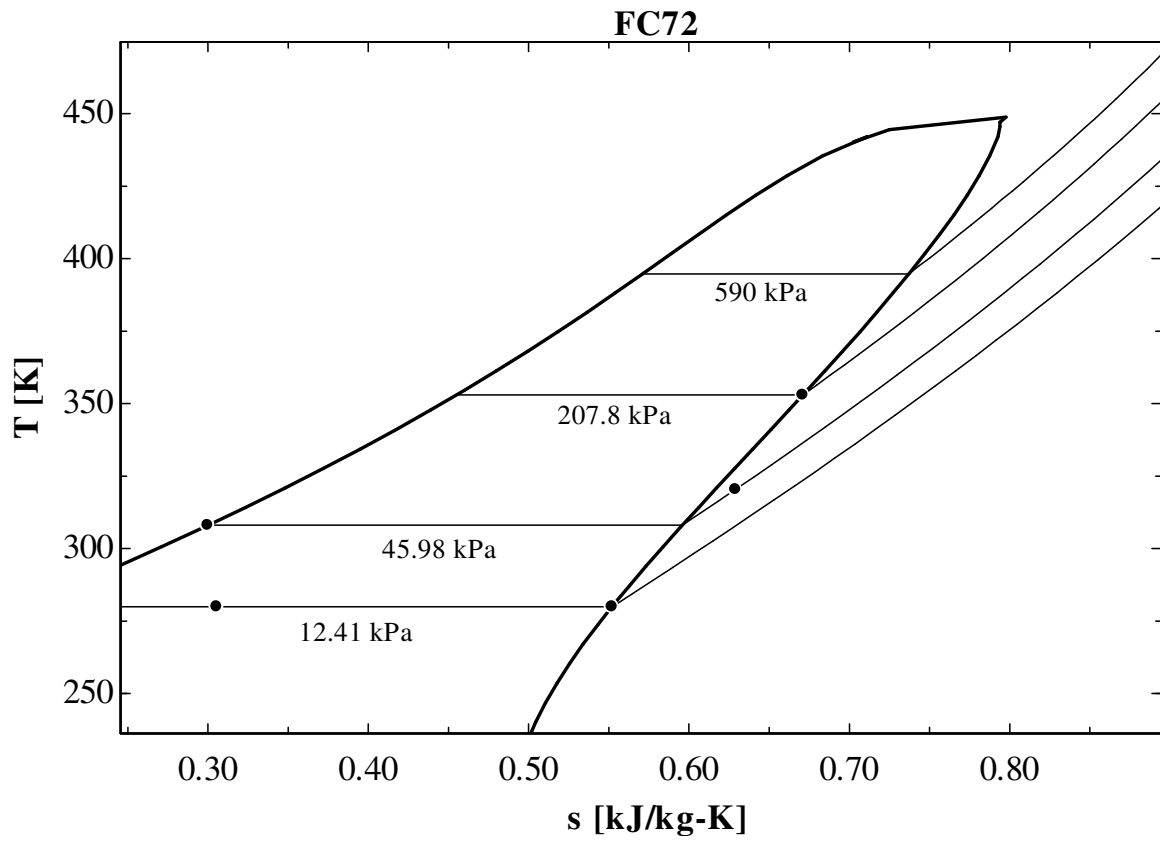


Figure 14. T-s diagram for FC72, highlighting the similar trends and state locations to R11

In all cases, the temperature of the outlet (State 3) falls in the expected range and the results agree well. These fluids will be examined below and one fluid will be chosen to complete the study. As previously noted, the model is flexible enough to allow for consideration of other fluids should it become necessary.

## 2.8 Working Fluid Selection Process

In order to identify an appropriate working fluid, a comparison study was conducted with all five potential fluids. The goal of this comparison is to examine the coefficient of performance (COP) and the maximum ejector diameter over the range of temperatures seen in the data center. The original goal of this system is to operate around temperatures of 100 °C, however to be applicable to the current data center environment a lower operating temperature of 50 °C should be considered. For that reason, the five working fluids are examined at 10 °C temperature increments between 50 °C and 80 °C. The first measurement under consideration is the size of the ejector. This measurement is defined as the diameter of the secondary flow, or opening 2 in Figure 8. This size is proportional to the entrainment rate, the generator and evaporator pressures and temperatures as seen in Equation 23. Each fluid is evaluated over the given temperature range, with a fixed condenser temperature of 308 K and fixed evaporator temperature of 280 K. Figure 15 presents the diameter change for each fluid.

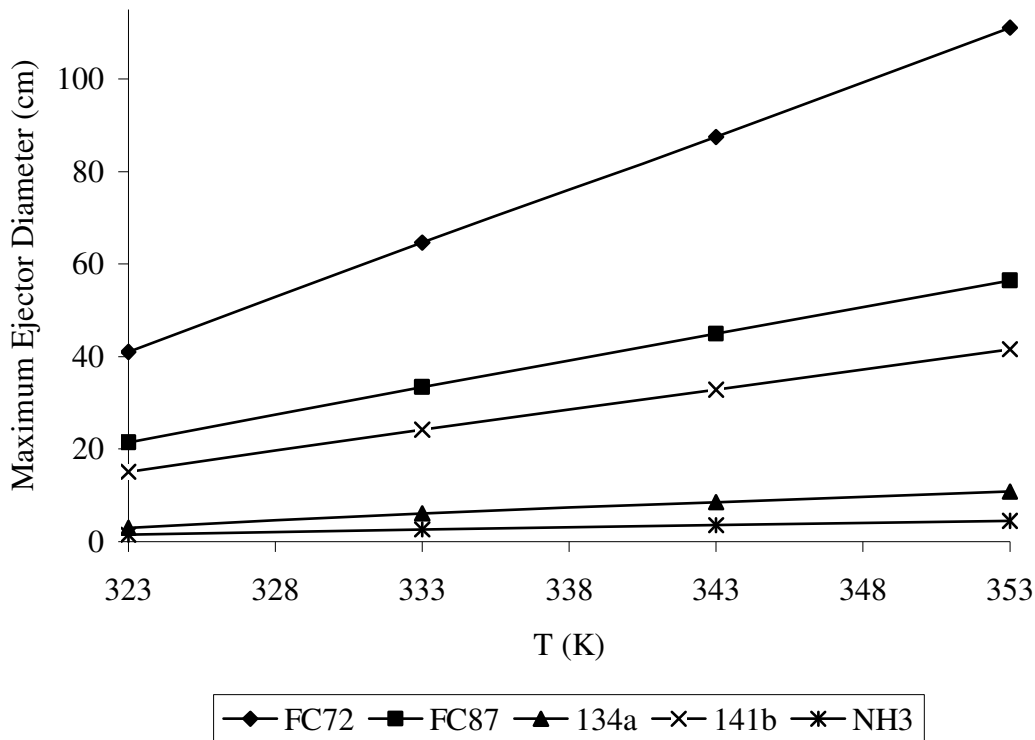


Figure 15. Change in ejector diameter over given temperature range

For the data center application, size is almost as important as the coefficient of performance of the system. Since the point of application will be inside the data center, the ejector component can not disrupt the operation of the data center. After examining the data from Figure 15, it can be seen that FC87 and FC72 require a large ejector and may not be suitable for this application. Furthermore, over the temperature range there is a very large increase in area size. This would limit the feasibility and scalability of the ejector in a data center environment where space and density are of great importance. From this study it appears that R-134a and Ammonia exhibit characteristics that are favorable to this application. Both fluids undergo a small increase in diameter over the range of temperatures and both never reach a

diameter size greater than around 10 cm. The next measurement compares the performance of the working fluids in this system.

### 2.8.1 COP Comparisons

The same conditions are used to evaluate the COP of each fluid. Figure 16 below presents the change in COP as the generator temperature is increased.

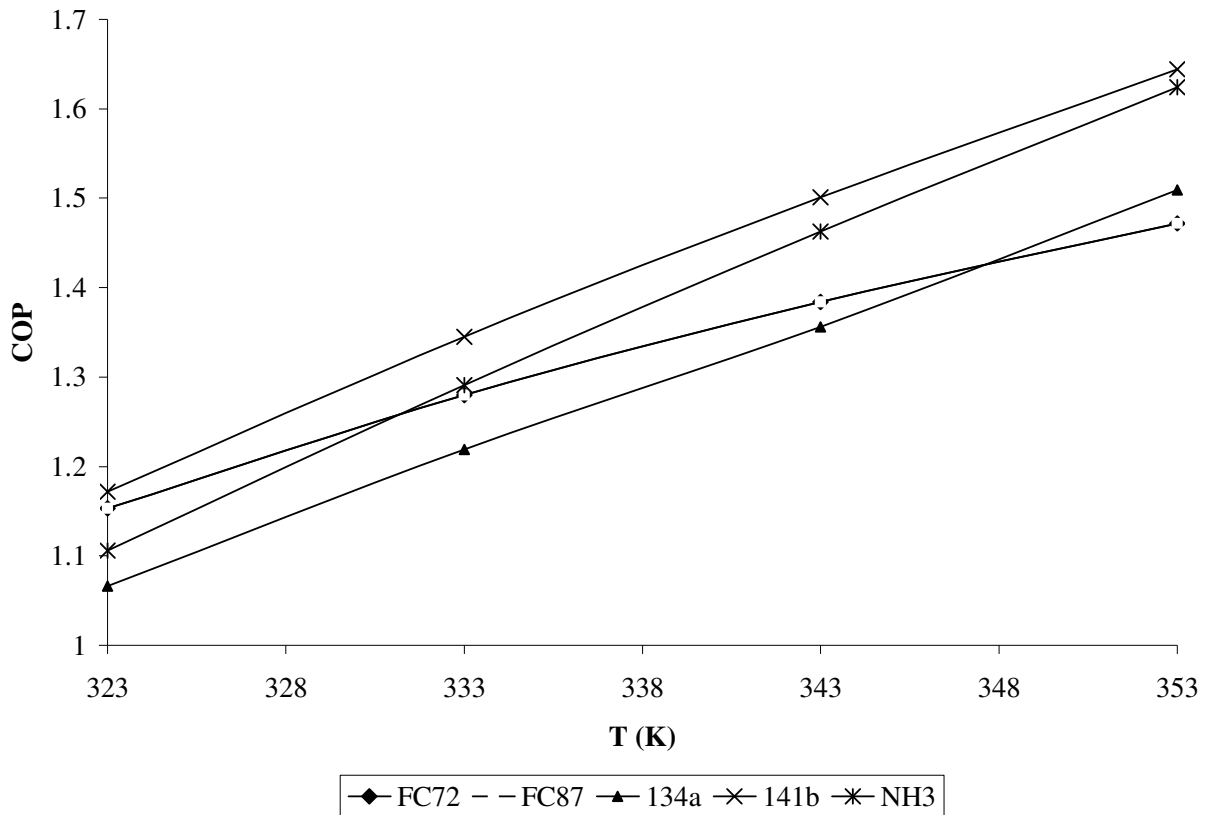


Figure 16. Change in COP over given temperature range

For this comparison, the goal is to have the highest COP value over the given temperature range. Each fluid shows an increase in COP as the temperature increases. From an examination of this data, it appears that R-141b exhibits the best overall COP, ranging from 1.17 – 1.64. The

next best fluid is Ammonia with a similar range of 1.11 – 1.62. Both of the FC fluids exhibit very similar COP's but fall short of R-141b and NH<sub>3</sub>. However the FC fluids do better than R-134a.

To effectively compare the fluids with both considerations a weighted scoring matrix is used. Since the size consideration is slightly more important than the performance, it is given a 60% weight and the COP a 40% weight. In each consideration there are two equally important factors, the performance at low temperatures and the increase over the temperature range. In order to use this system in the current data center environment, it is important to have effective performance in a temperature range of 50 °C to 100 °C. The increase in the metric over the given range indicates the effect of scaling and demonstrates its ability to perform at temperatures beyond the given range.

To formulate the diameter score, the difference between the diameter at 323K and 353K has been normalized against the largest difference. The second component is the low temperature performance so each diameter has been normalized by the largest diameter at 323K. Each of these components are equal weight so the normalized scores are combined and normalized again by dividing by two. Since a large diameter is a negative attribute, the normalized score is subtracted from 1 to give a higher score to the fluid with the least amount of diameter change.

To formulate the COP score a similar approach is used. Again, the current low temperature behavior is considered equally important to the increase in COP over the temperature range. In this case, the maximum difference and low temperature performance is normalized by the single greatest value in each category. These two scores are then summed and

normalized by 2. This yields their score on a scale between 0 and 1 and gives their relative strength against each working fluid.

The diameter score and the COP score are then multiplied by their weight factor to yield the fluid strength order. The scores and totals are presented below in Table 6. “S1” indicates the normalized score for the maximum difference and “S2” represents the normalized score for the low temperature performance.

Table 6. Fluid Scoring Matrix

COP Score					
	FC72	FC87	R-134a	R-141b	<i>NH3</i>
S1	0.556	0.616	0.855	0.911	<b>1.000</b>
S2	0.975	0.984	0.910	1.000	<b>0.944</b>
COP Rating	0.766	0.800	0.882	0.956	<b>0.972</b>
Diameter Score					
	FC72	FC87	R-134a	R-141b	<i>NH3</i>
S1	1.000	0.500	0.112	0.379	<b>0.042</b>
S2	1.000	0.521	0.073	0.367	<b>0.037</b>
Diameter Rating	0.000	0.489	0.907	0.627	<b>0.960</b>
Final Rating	<b>0.459</b>	<b>0.676</b>	<b>0.892</b>	<b>0.824</b>	<b>0.967</b>

Based on the results from the comparison matrix, Ammonia is the clear winner. As previously discussed this ejector system is based on steam models and Ammonia exhibits similar vapor dome properties. Also of note is the fact that the other refrigerants discussed are close behind the score of Ammonia, and FC72 and FC87 lag far behind. It is possible that the unique fluid properties of the FC group make it unsuitable for this application. Further study is suggested to examine other possible fluids. As previously demonstrated the fluids are interchangeable with favorable and reasonable results. If other fluids are to be considered in the

future, this model will still be valid. For the purposes of this study, Ammonia will be the chosen working fluid and further modeling will be considered with Ammonia only.

### 3. RESULTS AND DISCUSSION

#### 3.1 Baseline Conditions

Now that the working fluid has been identified, a baseline system will be examined and then parametric conditions will be varied and the system response studied. The baseline conditions are defined as follows in Table 7.

Table 7. Baseline operating conditions for the ejector heat pump system.

Generator Temperature	323 K
Evaporator Temperature	280 K
Condenser Temperature	298 K
Generator Heat Load	30 kW

The generator temperature is an achievable temperature in the near future. Furthermore, as previously demonstrated the system become more efficient as this temperature is raised. This is a temperature that can be controlled by controlling the outlet pressure of the boiler. Currently there are rear door heat exchangers that operate in similar conditions.

The evaporator needs to be cold but not so cold that it frosts up the coils. This temperature will vary with inside air temperature and flow rate. Controlling the fan speed is the means of changing the evaporator temperature. The condenser temperature will vary with the outside air temperature and air flow rate. This also directly affects the ejector performance, as the pressure of the condenser is the required exit pressure of the ejector component.

The generator heat load determines the size of the system. Based on the designed boiler heat transfer, this affects the ejector dimensions and the mass flow rate of the system. The rate of heat transfer in the boiler is a function of temperature and flow rate of the coolant bringing

heat to the boiler, and the temperature and flow rate of the working fluid coming to the boiler. This can be controlled by varying the pump in the system.

From Section 2.3 a detailed discussion on the effect of the ejector geometry was presented. The conclusion was that there exists an ideal geometry based on the initial conditions. However for the purpose of designing working systems it is not practical to vary the ejector geometry each time the operating conditions change. Therefore the baseline conditions will be used to find the appropriate geometry. Then the geometry will be kept fixed and the parametric conditions varied. Since the entrainment rate is directly proportional to the COP, the goal is to design for the maximum entrainment rate and set the geometry accordingly.

### 3.2 Geometric Relationships

The fixed areas are based on the initial, ideal system conditions in Table 7. The designation is “A-323” to indicate that the area is fixed to the generator temperature of 323 K. As different generator temperatures are used, the three digit number will adjust accordingly. Table 8 presents the ideal geometric relationships.

Table 8. Specified ejector geometry based on the ideal, initial conditions presented in  $\text{cm}^2$

$A_t$	2.472
$A_d$	8.733
$A_{np}$	3.995
$A_{ns}$	8.693

Figure 17 below shows the change in  $A_d$  based on varying either the condenser or the generator; this plot also shows the departure from the ideal ejector geometry.

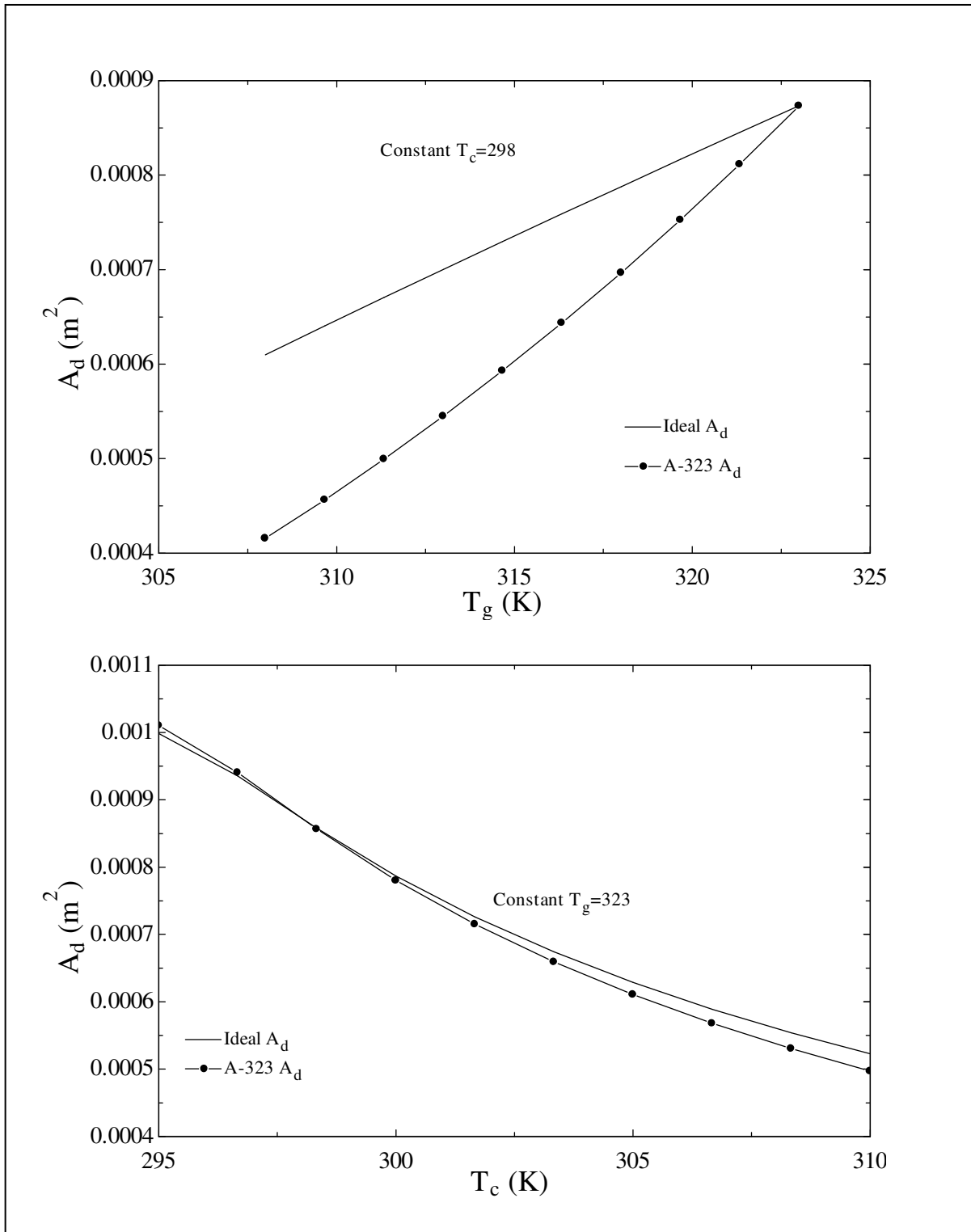


Figure 17. Deviation between ideal and fixed geometry for  $A_d$

As previously explained, when Region I is fixed, Region II needs to vary. This means that  $A_d$  will be allowed to vary with the change in initial conditions. The idea is to limit that variation. Notice that the relative change is nearly twice the area, but it is only a  $.0005 \text{ m}^2$  change. The two curves on the left represent when the generator is held constant and the condenser temperature is varied. The baseline and fixed area curves don't change much, indicating that the condenser temperature is a weak factor in determining  $A_d$ . On the right, a major difference is seen when the generator temperature varies. This indicates that the ejector should be run for a relatively fixed generator temperature.

Figure 17 shows that once the baseline geometry has been set, the boiler temperature should be maintained for a fixed condenser temperature. Thus the variation can only occur as the boiler temperature is lowered. This indicates that there is a maximum boiler temperature rating for specific ejector geometries.

The minimum functional operating characteristic for the ejector comes from the evaporator and "break-back" conditions. If the primary motive stream decreases too much a point is reached at which the ejector reaches "break-back" and ceases to operate [27]. This occurs when the generator temperature and pressure are too low depending on the particular fluid conditions. However, the temperature limit imposed by the evaporator is higher and therefore "break-back" is not a concern in this application. For a given geometry the evaporator temperature is lowered as the condenser temperature is held constant and the generator temperature is lowered. At a particular generator temperature the evaporator temperature will go below 273 K and freezing may occur for water. Figure 13 indicates the allowable points for a fixed geometry based on an initial generator temperature of 323 K.

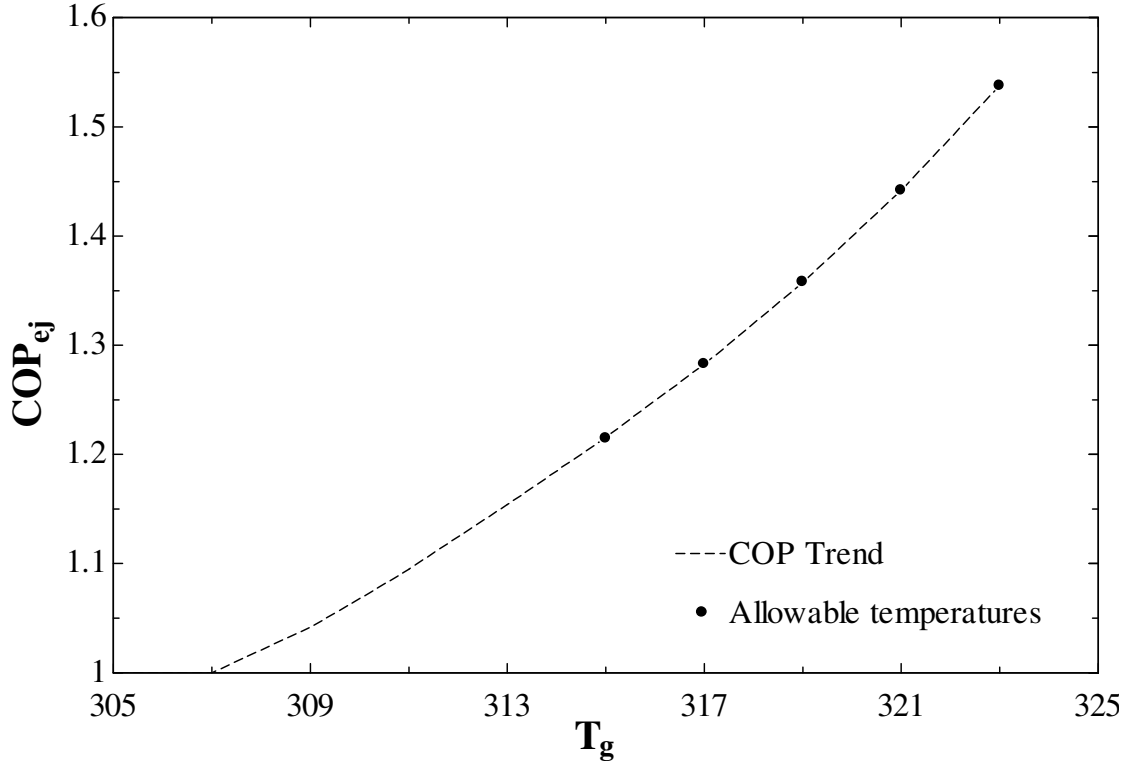


Figure 18. Allowable generator temperature range before freezing of the evaporator will occur.

Thus for a fixed geometry relationship in Region I, the generator is bounded by an upper and lower temperature. Based on this observation, further results will be found using fixed generator temperatures at 333 K, 323 K and 308 K. For each of these maximum generator temperatures the ejector geometry and the minimum temperatures are presented in Table 9.

Table 9. Ejector geometry for fixed generator temperatures, presented in  $cm^2$

$T_g$ [K]	$T_{min}$ [K]	$A_t$ [ $cm^2$ ]	$A_{np}$ [ $cm^2$ ]	$A_{ns}$ [ $cm^2$ ]	Total Length <sub>min</sub> [m]	Total Length <sub>max</sub> [m]
<b>308</b>	305	3.627	4.741	1.145	0.2794	0.5802
<b>323</b>	315	2.472	3.995	8.693	0.2306	0.479
<b>333</b>	324	1.96	3.659	15.17	0.2054	0.4265

The dimensions in Table 9 are small enough that fitting this system in and around the data center equipment is feasible. The standard data center tile is about 0.3 m in each direction. Therefore the largest ejector would be about 2 floor tiles long.

### 3.3 Coefficient of Performance Relationships

The performance of an ejector heat pump is highly dependent on the ideal operating conditions. Any deviation from these conditions relate to a dramatic decrease in performance. Figure 19 illustrates the difference in allowing the system to adjust for the optimum area, thus creating an ideal COP and fixing the area based on different  $T_g$  set points.

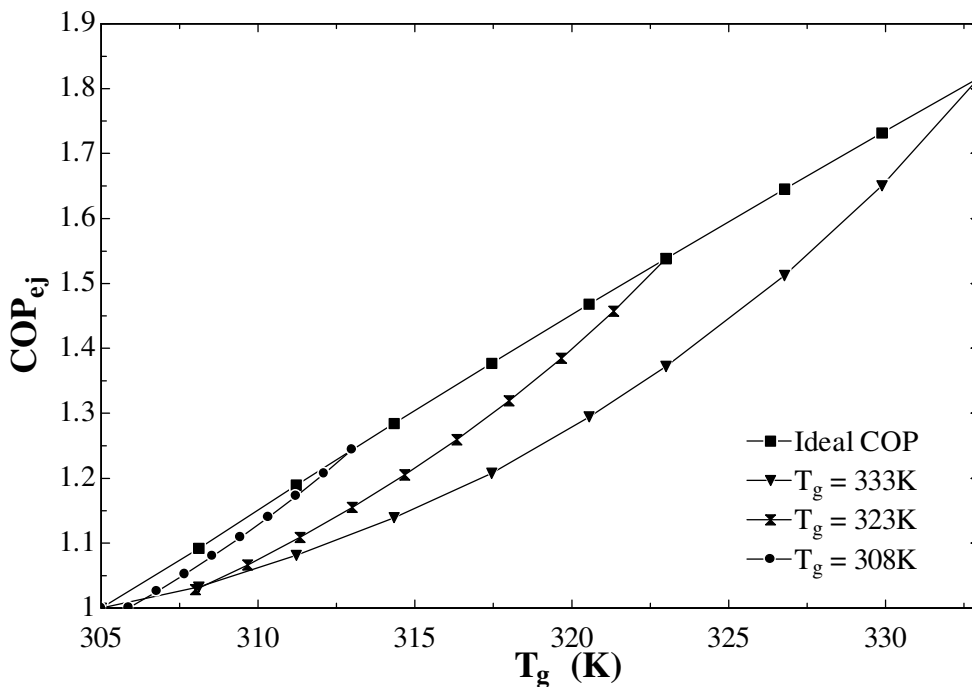


Figure 19. Deviation from ideal COP as the generator temperature is reduced.

From Figure 19, it can be seen that there is a dramatic reduction in COP as the area is fixed for a particular  $T_g$ , and  $T_g$  is subsequently reduced. This highlights the dependence of ejector area and importance on running the system at the designed generator temperature.

Now that the effect of the generator is known, an examination is conducted on the effect of the condenser.

The condenser temperature has two limits based on operating conditions. There exists an upper limit from the lack of temperature difference to effectively reject the heat to the ambient air. The lower temperature limit exists from the fact that the system can only achieve a particular maximum entrainment ratio based on the specified geometry of the ejector and condenser pressure. If the system code is left completely unconstrained to find its own ideal geometries, the ideal maximum entrainment ratio increases as the condenser temperature (and related Saturation Pressure) decreases. This continues until a maximum entrainment ratio is limited by the post-Normal-shock pressure.

The post-shock-pressure,  $P_y$  is related to the condenser pressure,  $P_c$ .  $P_y$  is expanded through the diffuser to match the condenser pressure as displayed originally in Equation 20 and reproduced below in Equation 33.

$$\frac{P_c}{P_y} = \left( \left( \frac{\eta_{diffuser} \cdot (k-1)}{2} \right) \cdot M_y^2 + 1 \right)^{\frac{k}{k-1}} \quad 33$$

After the two streams mix, they must enter the constant area mixing chamber with supersonic flow,  $M_x > 1$  to achieve shock and an increase in pressure across the mixing chamber. While  $M_x > 1$ ,  $M_y < 1$  as seen originally by Equation 17 and reproduced in Equation 34.

$$M_y^2 = \frac{M_x^2 + \left( \frac{2}{k-1} \right)}{\left( 2 \cdot \frac{k}{k-1} \right) \cdot M_x^2 - 1} \quad 34$$

The opposite relationship exists between the pressure pre and post shock as seen in Equation 35.

$$\frac{P_y}{P_x} = \left( \frac{1 + k \cdot M_x^2}{1 + k \cdot M_y^2} \right)$$

35

Because of the relationship between  $P_y$  and  $P_c$  there exists a minimum condenser pressure and temperature for the ejector, independent of the generator temperature. The condition that  $M_y$  cannot be greater than 1 fixes  $M_x$  and therefore for the system code to compile, the entrainment ratio is adjusted based on the generator temperature. Given that  $M_y \leq 1$ , the minimum condenser temperature is around 297 K and 550 kPa. At these conditions the system will produce a maximum entrainment rate based on a given generator temperature. This relationship and the entrainment values are displayed in Figure 20.

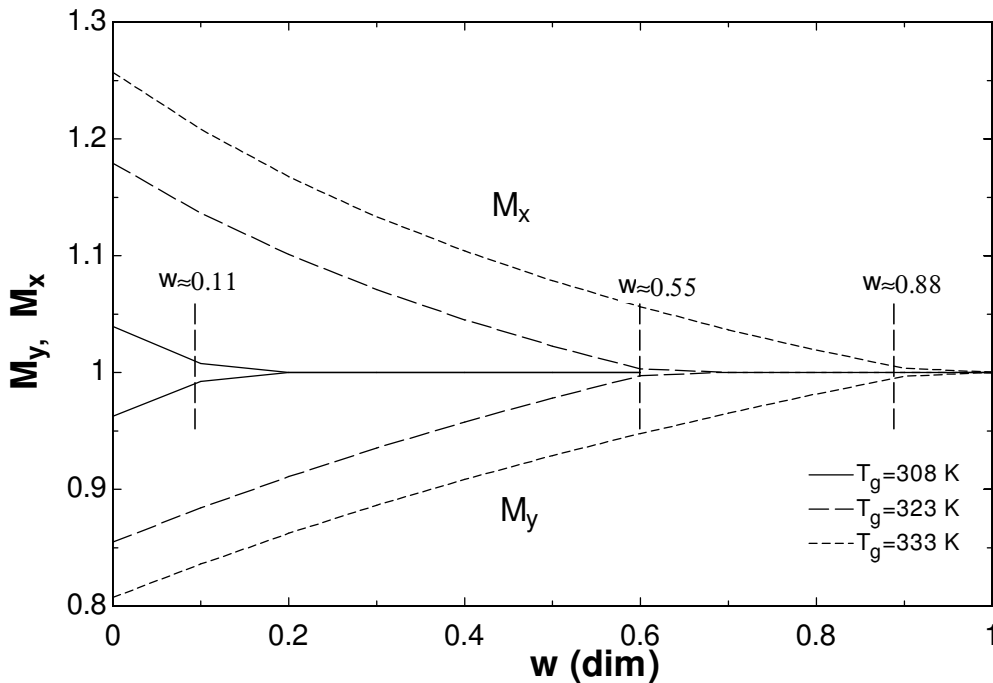


Figure 20. Maximum Entrainment Ratio for a given generator Temperature.

Under the baseline conditions from Table 7, there exists a fixed entrainment ratio. As the condenser temperature decreases, the ejector system cannot pull more than the fixed entrainment ratio and there is an excess wastage of vapor. This is confirmed by a study conducted by Munday and Bagster. In this study it is said that the system should be designed for the highest condenser pressure. Then under colder ambient conditions, the motive stream flow rate must be reduced in order to eliminate waste [28] of mechanical energy. If the motive stream's pressure is not reduced there will be excess pressure at the outlet of the ejector.

For the data center application, a reduction in the motive stream flow rate would come at the cost of waste heat removal from the data center. It is the goal to have a maximum entrainment ratio and that occurs at the lowest possible condenser pressure. Also, as sonic conditions are approached the losses from shock are reduced.

For the data center application, a new design parameter should be developed, distinct from Munday and Bagster. Based on the data presented from this study, the system should be designed for maximum entrainment ratio and the excess pressure bled off if the ambient temperature drops below the design parameter.

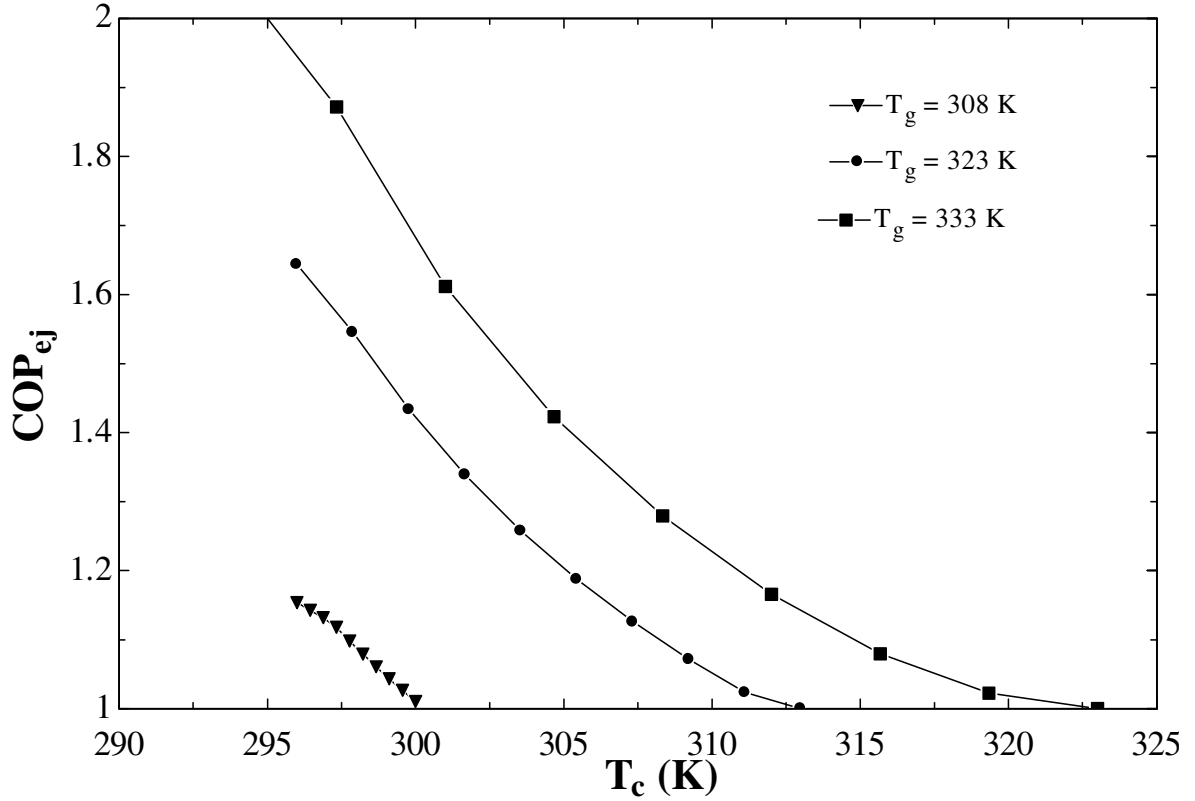


Figure 21. Maximum attainable COP given a rise in  $T_c$

At approximately 295 K or below the maximum COP for each generator temperature is reached. The correct original design of the ejector geometry will prevent too much excess pressure. From Figure 16, the system then can handle an ambient rise up to about 10 K below the generator temperature. The maximum COP's for each generator temperature is provided below in Table 10.

Table 10. Maximum COP for given generator temperatures

$T_g$ [K]	COP
333	1.818
323	1.538
308	1.088

### **3.4 Economic Analysis**

In order to evaluate the competitiveness of this model system, some basic economic estimates are considered. Since this is a new approach currently available components may not match the requirements of the system. In these cases every effort has been made to compare to a related component currently in production. To evaluate the equipment necessary for an economic analysis a baseline 1 Mega-Watt data center is discussed. This is followed by the size and cost of the equipment necessary to compare the components of this model with a vapor compression system.

#### **3.4.1 1 MW Data Center Size Considerations**

As computers and servers evolve the datacenter density is increasing. However, the objective in cooling is to keep the temperature difference across the server around 15 °C, as seen in various data center applications [29]. For the foreseeable future this “Delta T” will hold and the model data center will reflect a 15°C delta T across the server racks. As previously stated, data center racks are approaching 30 kW and are expected to increase [2]. The model 1MW data center will consist of 30 racks with a heat load of 35 kW for a total load of 1.05 MW. The goal of this study is to create a control volume with global details, not to concentrate on air flow patterns or server arrangements. Therefore this data center will assume a hot and cold aisle arrangement as discussed in Intel’s study [29].

In order to estimate the size of the components in the proposed cooling system, the required airflow for the 1 MW data center is calculated. Taking the server as the control volume, the required air flow for each server is calculated from Equation 36 and converted to Cubic Feet per Minute (CFM) by Equation 37 [30].

$$\dot{m} = \frac{Q}{C_p \Delta T} \quad 36$$

$$\text{CFM} = \dot{m} \cdot \frac{1}{\rho_{air}} \quad 37$$

Given the constants in Table 11, below, the results in Table 12 provide the 1 MW data center baseline information.

Table 11. 1 MW Data center baseline variables for each server rack.

Variable	Value	Units
Q	35	kW
$c_p$ (air)	1.004	kJ/kg-°C
$\Delta T$	15	°C

Table 12. Flow rate per rack for a high density 1 MW data center.

Baseline Quantity	Value
$\dot{m}$	2.32 kg/s
CFM	4,090

The information in the above tables will provide a general guideline as to the size requirements of the ejector model components. Given the varied nature of data center cooling systems it is extremely difficult to predict and generalize the install cost of a particular system. Instead, a general estimate as to the cost and size of the ideal system is given.

### 3.4.2 Size and Cost of Ejector Model Components

The main cost considerations in this ejector heat pump are in the components that replace the compressor in a traditional vapor-compression refrigeration system. These components are

the ejector component, heat exchanger/boiler and the pump. In comparing the cost to a traditional system, this will be the main benchmark.

### **Ejector Component**

As noted in Section 2.3, the ejector size doesn't change significantly given a larger heat load. The ejector relies on a high pressure vapor to enter in order to entrain the secondary vapor. This allows for a single ejector for the entire system. As long as the pressure and temperature can be achieved to vaporize the Ammonia, a single ejector can handle the load. There are very few ejector manufacturers in operation at the time of publishing; however one ejector manufacturing company estimates the ejector design to be \$4,000 [32].

### **Heat Exchanger/Boiler**

The heat exchanger component is a very common device, but a challenge for this application. In order for the Ammonia to vaporize at 50 °C it requires 2026 kPa of pressure. This value is higher than most typical heat exchanger applications and makes cost estimation difficult. One company contacted specializes in high pressure heat exchangers [33]. They were able to provide some cost data that can be expanded upon along with some basic heat transfer equations to get an estimate of the heat exchanger cost. In addition, the IBM Rear Door Heat Exchanger serves as a current industry baseline.

Because of the uncertainty in the server outlet conditions and the lack of experimental data, the effectiveness-NTU method is applied. This is preferred method for existing heat exchangers and can be easily expanded to give an estimate of the heat exchanger needed for this ejector heat pump. The IBM system claims a 55% capture of heat from a high density rack and has a retail cost of about \$4,300 [17]. This can be used as a potential effectiveness rating and its associated NTU. The information provided by the manufacturer of the heat exchanger coil gives

an effectiveness rating of about 86% when a 30 kW heat load is provided to the designed coil with the raw coil cost at \$1,100. This system requires an air flow of 1,000 CFM and as a face area of 0.201 m<sup>2</sup>. The effectiveness and cost data is summarized in Table 13.

Table 13. Baseline cost and effectiveness data for heat exchanger analysis.

	<b>IBM Heat Exchanger</b>	<b>Super Radiator Coil</b>
<b>Effectiveness</b>	0.55	0.86
<b>Unit cost</b>	\$4,300	\$1,000

This design will be a single pass cross flow heat exchanger. In order to use the effectiveness model, the heat capacity rates need to be determined. Equation 38 is used to calculate  $C$ , the heat capacity rate for the cold and hot sides of the exchanger. The air side is considered the hot side and the Ammonia in the coil is considered the cold side.

$$\begin{aligned}
 C_h &= \dot{m}_h c_{p,h} \\
 C_c &= \dot{m}_c c_{p,c}
 \end{aligned}
 \tag{38}$$

This particular heat exchanger will serve as a boiler and therefore a phase change will take place between the fluid inlet and vapor outlet. This will make the heat capacity rate infinite on the cold side. Using the data from Section 3.4.1 Equation 39 demonstrates the hot and cold side heat capacity rates.

$$\begin{aligned}
 C_h &= \left( 2.32 \frac{\text{kg}}{\text{s}} \right) \left( 1.004 \frac{\text{kJ}}{\text{kg} \cdot \text{C}} \right) = 2.329 \frac{\text{kW}}{\text{C}} \\
 C_c &= \infty
 \end{aligned}
 \tag{39}$$

The next important parameter is  $C_r$ , the heat capacity ratio. This ratio is necessary to use the effectiveness-NTU equations for various heat exchanger arrangements. The heat capacity ratio is determined by Equation 40.

$$C_r = \frac{C_{\min}}{C_{\max}} \quad 40$$

Where  $C_{\min}$  and  $C_{\max}$  are assigned the values of  $C_h$  and  $C_c$  depending on their relative magnitudes. In this particular case,  $C_r$  is equal to zero because  $C_{\max}$  is considered infinite due to the phase change. In this scenario, the heat exchanger behavior is independent of flow arrangement and holds for all types of heat exchangers. The appropriate effectiveness-NTU equation is displayed as Equation 41 [31].

$$\varepsilon = 1 - e^{(-NTU)} \quad 41$$

This equation requires a particular effectiveness value and returns the NTU value. The NTU value is related to UA, a basic measure of the size of a heat exchanger. The UA value is product of the total heat transfer coefficient and surface area of the heat exchanger. This relationship is demonstrated in Equation 42.

$$NTU \equiv \frac{UA}{C_{\min}} \quad 42$$

The baseline data from Table 13 will be used to create a low and high limit to the NTU value as well as the UA value and is presented in Table 14. The value to be used for  $C_{\min}$  has been calculated in Equation 39.

Table 14. NTU and UA range for heat exchanger sizing.

	<b>Effectiveness</b>	<b>NTU</b>	<b>UA [kW/°C]</b>
<b>Upper Limit</b>	0.86	1.966	4.579
<b>Lower Limit</b>	0.55	0.798	1.859

The values presented in Table 14 are for the individual rack level heat exchanger sizes. The heat load is distributed at the rack level, and the heat exchangers will be at the rack level. These values can be used to estimate the number of the heat exchanger required to provide cooling to a 1 MW data center.

This ejector heat pump has a COP larger than 1 so it will not require a large effectiveness value. The maximum COP value at 323 K presented in Table 10 is 1.538. Based on this value in order for the system to provide 1.05 MW of cooling, the boiler will only require 650 kW as demonstrated in Equation 43.

$$BoilerLoad = \frac{TotalLoad}{COP} = \frac{1050 \text{ kW}}{1.538} = 650 \text{ kW} \quad 43$$

This load can be distributed over the 30 racks as the required load into the heat exchangers or using the  $UA$  of the baseline systems a number of required heat exchangers can be determined.

Using the equal distribution method, this yields a load of 21.7 kW per heat exchanger located at the back of each high density server rack. The 21.7 kW load into the heat exchangers relates to 62% of the available 35 kW load for each server rack. This effectiveness value falls in the range of baseline products and is reasonable for this application.

Using the  $UA$  method the effectiveness of the heat exchanger is assumed to be 62% since 650 kW of 1050 kW is required. Using Equation 41 the associated NTU value is 0.967. Taking  $C_{min-room}$  as thirty times the rack level,  $C_{min-room} = 30 \cdot C_{min} = 69.87 \text{ kW}/^{\circ}\text{C}$  the room level required  $UA$  is calculated using Equation 42. The resulting room level  $UA$  is calculated to be 67.6 kW/ $^{\circ}\text{C}$ . This value is then divided by the upper and lower  $UA$  values to calculate the number of heat exchanger units necessary to deliver the required load. This represents 15 units

at the upper level value and 38 units at the lower value. Since the equal distribution required only 30 units, this will be taken as the maximum number of heat exchangers and the 38 value will not be considered.

The manufacturer provided the raw cost of the heat exchanger coil [33]. This did not include the controls or housing required for the complete heat exchanger. To compensate for the lack of a complete unit and the additional material to handle higher pressures and CFM, the quoted price will be raised by 50% and estimated at a cost of \$1,650 per unit. This is a reasonable assumption at about 40% of the IBM unit cost, since this heat exchanger represents one component and not a completed unit. The total cost of 30 units based on the equal distribution method will be estimated at \$49,500. Using the *UA* scaling method, 15 units will cost \$24,500. Using the two methods' values, a range of \$49,500-\$24,500 is estimated for the total cost of the heat exchanger component.

### **Pump**

Similar to the ejector component, there will be one centralized pump, right before the heat exchanger arrangement. This will control the entire system and will raise the liquid Ammonia to the appropriate saturated vapor pressure according to the boiler heat load. Currently there are providers of liquid ammonia pumps capable of 400 psi or 2758 kPa [34]. This is larger than the 2026 kPa required. This pump is large enough to overcome the pressure loss over each heat exchanger. The heat exchanger coil manufacturer states that the pressure drop over each coil is about 0.7 kPa for a total of 21 kPa pressure loss [33]. This amounts to a pumping need of 2047 kPa which is less than the pump can provide. A distribution company of sells the pump at \$3,500 [35].

The three main component costs are summarized in Table 15. Because of the varied nature of data center cooling it is difficult to compare install costs and applications. The information from this chart will be used to compare the ejector heat pump to a comparable compressor.

Table 15. Total ejector heat pump system cost breakdown.

<b>Component</b>	<b>Quantity</b>	<b>Unit Cost</b>	<b>Total Cost</b>
Ejector	1	\$4,000	\$4,000
Heat Exchanger/Boiler	15-30	\$1,650	\$24,500-\$49,500
Pump	1	\$3,500	\$3,500
Total System Cost			<b><i>\$32,000-\$57,000</i></b>

### 3.4.3 Comparison with a traditional vapor-compression system

In order to provide cooling in a traditional vapor-compression refrigeration system, the work into the system is consumed by the compressor. Vapor compressors are much less efficient than liquid pumps and represent the most expensive component of the vapor-compression refrigeration system. For the 1 MW data center application an 86 kW compressor is necessary to provide the same cooling as the ejector heat pump. This load requires a 150 HP compressor and they retail for \$46,000 [36]. This gives a good capital cost comparison to the ejector heat pump. The main system component capital cost comparison is displayed in Table 16.

Table 16. Capital cost comparison for ejector heat pump and vapor-compression refrigeration.

Ejector Heat Pump Components	\$32,000-\$57,000
Vapor- Compression System Compressor	\$46,000

From the estimates given, the two systems are comparable in initial capital cost. The ejector heat pump has a larger range because of the design uncertainties in the cost estimate. Even at the higher initial cost, the system still remains competitive especially when operating cost is considered.

The same expected operating conditions are used to compare the electrical performance of the two systems. At the time of this paper, the national commercial use average cost of electricity is \$0.0977 per kW-hr [37]. The cost to run the systems needs to be considered when examining the two systems. The operating time of the compressor is assumed to be 50%, or 12 hr a day. This accounts for the cycling of the system. In order for the ejector heat pump to function, the pump needs to run 24 hrs a day. These run times are considered when comparing the annual cost of electricity. Table 17 shows the comparison data.

Table 17. Ejector and Vapor Compression System cost comparisons

<b>Metric</b>	<b>Ejector System</b>	<b>Vapor Compression System</b>
<b>COP</b>	1.538	11.53
<b>W [kW]</b>	0.94	87
<b>Annual Electrical Consumption [kW-hr]</b>	8,234.4	381,060
<b>Annual Cost of Electricity</b>	\$804.5	\$37,229

The immediate impact on the cost savings is seen in the reduction of operating cost for the year. The ejector heat pump shows a \$36,425 cost savings when considering the electricity consuming devices.

The Coefficient of Performance for the Vapor Compression system is still significantly greater than that of the Ejector Heat Pump System. This is to be expected; however, the required amount of work to run the compressor is much greater than the Ejector Heat Pump and indicates a higher cost to run the system. Since the goal of this design study is to improve Power Use Effectiveness in a data center, the most important factor is the amount of electricity that is dedicated to cooling. The fact that the electricity needed is a factor of 100 less than a traditional vapor compression cycle demonstrates the fact that this system has potential applications in the data centers. Since the waste heat is free, the only investment in this system is the initial capital cost and a minimal amount of pump work. This proves that an Ejector Heat Pump is a feasible alternative to data center cooling.

## 4. CONCLUSIONS

An examination of possible low grade, waste heat engines was conducted to identify a viable technology for waste heat recovery in the data center. The thermoelectrics had too low of an efficiency to justify their costs. The phase change materials didn't support applicable improvements in PUE and the absorption systems were found to be difficult to scale for data center applications. This was followed by an examination of current cooling technologies. The purpose of this exercise was to identify reasonable operating conditions. Together, these background studies provided the necessary information to choose a viable technology for consideration. With the goal of improving the data center PUE, by using waste heat and reducing the electrical input, an Ejector Heat Pump was selected as the device to consider for further examination.

### 4.1 Design Recommendations

After performing all the analysis on the ejector heat pump there are some recommendations for the components of the system. The boiler temperature is needed to set the geometry relation for maximum COP. If the temperature is too high, the system cannot handle the pressure. If the generator temperature is too low, the evaporator runs the risk of freezing. Therefore the system needs to be designed with these limits in mind. Furthermore, the condenser limits need to be considered. There exists only one real limit, the maximum temperature at which there is no heat rejection. This is roughly 10 K below the generator temperature. The following steps are recommended for an effective evaluation of future ejector designs for a given set of ideal initial operating conditions.

1. Design for maximum entrainment rate
2. Find the lowest possible  $T_{c0}$  that ensures  $M_y \leq 1$
3. Specify an ideal maximum generator temperature,  $T_{g0}$
4. Specify the evaporator temperature,  $T_{e0}$
5. Run the model for the baseline conditions  $T_{c0}$ ,  $T_{g0}$  and  $T_{e0}$ , to find the maximum entrainment rate and ideal geometry.
6. Fix the proper geometric relationships.
7. Conduct off design studies to examine COP within the following limits
  - a.  $T_g$ : the maximum value is  $T_{g0}$ , the minimum  $T_g$  is based on keeping  $T_e$  above 273 K
  - b.  $T_c$ :  $T_{c0}$  represents the lowest  $T_c$  and maximum COP, so this is the minimum for study, the maximum value of  $T_c$  needs to be determined by thermodynamics.

## **4.2 Model Limitations**

It should be noted that the model presented for analysis is limited due to some of the assumptions and model simplifications made. Modeling ejectors using thermodynamic models presents some challenges and limitations with respect to the events taking place within the ejector component. Furthermore, a two dimensional model presents limitations in explaining the complex conditions inside the ejector. A detailed computational fluid dynamics study should be conducted to further examine this component.

Using the conditions in this analysis there exist some debate in how to model the mixing pressure in the ejector. To improve performance and model the second inlet as modeled as sonic and at choked flow. This occurs when the mixing pressure is lower than the evaporator

pressure and is modeled this way in the Alexis paper [20]. However, concerns exist about the manner to set the pressure lower than the evaporator. The Hsu paper [19] notes this issue by setting the ejector mixing pressure equal to the evaporator pressure. It is important to note that several options exist to model the ejector components and it is not the purpose of this thesis to determine the correct method to use. Instead, a model was selected which fit the conditions of the data center.

### **4.3 Model Improvements and Future Recommendations**

In proven ejector system model there was a lack of clear solutions for the geometry of the ejector component. This study attempts to determine more geometric parameters than previously done. Unfortunately, it falls short on determining one geometric relationship,  $A_d$ . This mixing chamber area needs further study to understand its affect on the COP of the system. An ideal solution would incorporate fixing this constraint and conducting the study again.

An experimental validation of the methodology is also considered vital. Initially some simple tests should be developed specifically on the ejector component to access its behavior experimentally, compared to its modeled behavior. After validating the ejector component, a scalable set-up should be implemented. Beyond the experimental validation of the system, a true cost model and comparison with existing technologies can be completed.

### **4.4 Ejector Heat Pump Conclusions**

A detailed mathematical model and accompanying EES code was developed to evaluate the Ejector Heat Pump. Based on previous studies, the model attempted to examine the effect geometry in off design conditions to develop some guidelines for the operation of the system's specific components. The entrainment ratio, and ejector geometry were allowed to adjust from

the baseline conditions of the system. This is unacceptable in the data center environment, and for possible deployment of this system. It is the conclusion of this study that the most important region of fixed geometry lays in the inlet areas of the ejector. Furthermore, the variation of the generator temperature has a larger negative effect on the area considerations than does the variation of the condenser. For future development of this model, it is suggested that a solution be presented for fixing all of the ejector geometries.

Once the relationship between performance and geometry was determined, the coefficient of performance was evaluated in off design variations. It was shown that the COP of the system is highly dependent on operating conditions. When deviating from baseline conditions, the condenser temperature had the greatest effect on COP. It was determined that for given generator and condenser temperatures there exists an optimum fixed ideal geometry. As the condenser temperature deviates from this baseline, the COP is reduced. As the condenser temperature decreases, the system reaches a maximum COP. The lowest condenser temperature is determined by finding the lowest allowable temperature that induces shock across the mixing section. The general operating conditions for the generator and condenser represent new limits not previously studied. These conditions are important for future development of this system.

The last major conclusion is the reduction in electrical input into this system. Given that the cost of “fuel” is free, the system doesn’t have to operate with large efficiencies to dramatically improve the PUE. It just needs to have a low electrical input. Compared to a similar vapor compression cycle, the Ejector Heat Pump requires 1/100<sup>th</sup> the amount of electrical input. This will dramatically improve the data center Power Use Effectiveness. Ultimately the Waste Heat Ejector Heat Pump provides an effective system to improve data center PUE and a novel solution to the initial design objective.

## INDIVIDUAL CONTRIBUTIONS

This thesis contains a novel approach to an existing idea. The idea of an ejector heat pump has been in existence for nearly a century. However, it remains an overlooked and under examined device in the realm of waste heat recovery. The purpose of this thesis was to identify a technology for use in a data center that would reduce the electric consumption through storage, energy generation or recovery of waste heat. This thesis examined several technologies that are being developed for other uses and examined their data center potential. It is the bringing together of these ideas and examining them with a new focus that stands as a unique contribution. The collection of industry leading cooling technologies and presenting them in this fashion also represents an individual contribution.

The thesis is then treated as a design project in fulfillment of the sponsor's wish of receiving preliminary research for development of a new device for data center cooling. The information on ejector theory is readily available and was helpful in developing the models, however many of the models have not been tested at the low-heat temperatures that the data center application requires.

In previous studies of ejector geometry there has not been an emphasis on fixing the geometric relationships of the ejector. These studies represent an idealized case of an ejector pump with several degrees of freedom. This thesis examines the relationships in system performance when certain geometric relationships in the ejector component are fixed. This is a new area of examination and represents the considerations required for physical development of this system.

Finally, the gathering of cost data for this particular system has not been done. The environmental dependence of data center cooling systems made collecting this cost data a

challenge so a comparison between the model components and an existing vapor-compression compressor has been examined. The estimates seem reasonable and complete the preliminary design study. The gathering of cost data applicable to this system has not previously been examined. The application of an ejector heat pump to a data center represents a unique contribution.

## REFERENCES

- [1] Hewlett-Packard Development Company. *Control power and cooling for data center efficiency: An HP BladeSystem innovation primer*. 4AA0-5820ENW, June 2006
- [2] ASHRAE, *Thermal Guidelines for Data Processing Environments*. ASHRAE. 2004
- [3] ENERGY STAR Program. Report to Congress on Server and Data Center Energy Efficiency Public Law 109-431. Environmental Protection Agency. 2007
- [4] The Green Grid. *The Green Grid Data Center Power Efficiency Metrics: PUE and DCiE*. The Green Grid. 2007
- [5] Sharma, S. D.; Sagara, Kazunobu. *Latent Heat Storage Materials and Systems: A Review*. International Journal of Green Energy 2.1 (2005). 2007
- [6] Inorganic Materials, 2007, Vol. 43, No. 9, pp. 933–937. Pleiades Publishing, Inc., 2007. Original Russian Text © L.D. Ivanova, L.I. Petrova, Yu.V. Granatkina, V.S. Zemskov, 2007, published in *Neorganicheskie Materialy*, 2007, Vol. 43, No. 9, pp. 1044–1048.
- [7] Fleurial, J.-P.; Borshchevsky, A.; Caillat, T.; Ewell, R., *New materials and devices for thermoelectric applications, Energy Conversion Engineering Conference, 1997. IECEC-97., Proceedings of the 32nd Intersociety*, pp.1080-1085 vol.2, 1997
- [8] Gao Min; Rowe, D.M., *Recent concepts in thermoelectric power generation, Thermoelectrics, 2002. Proceedings ICT '02*, pp. 365-374, 2002
- [9] Rowe, D.M.; Gao Min; Kuuleetsov, V.; Kaliazin, A., "Effect of a limit to the figure-of-merit on thermoelectric generation," *Energy Conversion Engineering Conference and Exhibit, 2000. (IECEC) 35th Intersociety*, vol.1, no., pp.128-134 vol.1, 2000
- [10] Herold, K.E.; Radermacher, R., *Integrated power and cooling systems for Data Centers, Thermal and Thermomechanical Phenomena in Electronic Systems, IThERM. The Eighth Intersociety Conference*, pp. 808-811, 2002
- [11] Rafferty, Kevin, *Absorption Refrigeration, Geothermal Direct Use Engineering and Design Guidebook*, Third Edition, Geo-Heat Center, Oregon Institute of Technology, Klamath Falls, OR. Ch. 13 1998.
- [12] M.Z.I. Khan, B.B. Saha, K.C.A. Alam, A. Akisawa and T. Kashiwagi, *Study on solar/waste heat driven multi-bed adsorption chiller with mass recovery*, Renewable Energy Volume 32, Issue 3, pp. 365-381. March 2007

- [13] Takahashi, Y.; Nishikawa, M., *Development of thermomagnetic engine for exhaust heat recovery, Magnetics Conference, 2003. INTERMAG 2003. IEEE International 2003*
- [14] TAKAHASHI YUTAKA. *Fundamental Performance on Disc Type Thermomagnetic Engine IEEE Transactions on Power and Energy* vol: 123 issue: 7 pp. 883-889. 2003
- [15] Rittal, *Perfect Cooling*, Rittal 2006
- [16] Niemann, John *Best Practices for Designing Data Centers with the InfraStruXure InRow RC*, APC 2006
- [17] IBM Systems and Technology Group, *Keeping Your Data Center Cool: There Is Another Way*, IBM 2005
- [18] Roger, Schmidt, Madhusudan Iyengar *Analytical Modeling of Energy Consumption and Thermal Performance of Data Center Cooling Systems – From the Chip to the Environment at IPACK2007*. IBM. 2007.
- [19] Hsu. *CT Investigation of an Ejector Heat Pump by Analytical Methods*. Oak Ridge National Laboratory. 1984.
- [20] Kouremenos, D.A, E.D. Rogdakis and G.K. Alexis. *Optimization of Enhanced Steam – Ejector Applied to Steam Jet Refrigeration*. Proceedings of the ASME Advanced Energy Systems Division **38** pp. 19-26 1998
- [21] J.H. Keenan, E.P. Neumann, F. Lustwerk, *An investigation of ejector design by analysis and experiment*, Journal of Applied Mechanics **72** pp. 299-309. 1950
- [22] Alexis, G.K., *Estimation of ejector's main cross sections in steam-ejector refrigeration system*. Applied Thermal Engineering **24** pp. 2657-2663. 2004
- [23] El-Dessouky, Hisham, Hisham Ettouney, Imad Alatiqi, Ghada Al-Nuwaibit. *Evaluation of steam jet ejectors* Chemical Engineering and Processing **41** pp. 551–561 2002
- [24] ASHRAE, *Steam-jet refrigeration equipment*, Equipment Handbook, **13** pp. 13.1–13.6. 1979
- [25] ASHRE, *Ammonia as a Refrigerant*, ASHRE. 2002
- [26] Campbell, Nick, *Responsible Refrigeration*, Chairman EFCTC. Dec. 2005
- [27] Stevens, R.H. “Characteristics of the Steam-Jet System.” Refrigerating Engineering. **40** pp. 149-151 1940.
- [28] Munday, John T. and David F. Bagster, *A New Ejector Theory Applied to Steam Jet Refrigeration*. Industrial and Engineering Chemistry. **16** pp. 442-449 1977

- [29] Garday, Doug and Daniel Costello, *Air-Cooled High-Performance Data Centers: Case Studies and Best Methods*, Intel Corporation 2006
- [30] Moran, Michael, and Howard Shapiro. Fundamentals of Engineering Thermodynamics, 5<sup>th</sup> Edition. Hoboken: Wiley, 2004.
- [31] Incropera, Frank, David DeWitt, et. Al. Fundamentals of Heat and Mass Transfer 6<sup>th</sup> Edition. Wiley. 2006.
- [32] *Croll Reynolds of New Jersey*, ejector manufacturer
- [33] *Super Radiator Coil of Richmond, Virginia*, heat exchanger coil manufacturer
- [34] *Buffalo Pumps of New York*, ammonia pump manufacturer
- [35] *Genemco of Bryan, Texas*, pump distributor
- [36] *Eaton Compressors of Ohio*, industrial rotary screw compressor manufacturer
- [37] Energy Information Administration, *Average Retail Price of Electricity to Ultimate Customers by End-Use Sector, by State*. April 2008
- [38] Harris, L.S., A.S. Fischer. "Characteristics of the Steam-Jet Vacuum Pump." Journal of Engineering for Industry 86 (1964): 358-364
- [39] Stevens, R.H. *Characteristics of the Steam-Jet System*. Refrigerating Engineering. 40 pp. 149-151 1940
- [40] Stoecker, W.F., and J.W. Jones. *Refrigeration and Air Conditioning, Second Edition*. St. Louis: McGraw Hill, 1982.
- [41] John, James. Gas Dynamics. Upper Saddle River: Prentice Hall, 1984.